

Birgit Unterweger

**PEGylation and characterization of
Aerococcus viridans L-lactate oxidase S218C
mutant**

Masterarbeit

zur Erlangung des akademischen Grades einer
Diplom-Ingenieurin

der Studienrichtung Biotechnologie
eingereicht an der
Technischen Universität Graz

Univ.-Prof. Dipl.-Ing. Dr.techn. Bernd NIDETZKY
Institut für Biotechnologie und Bioprozesstechnik
Technische Universität Graz

2011



*There is something fascinating about science.
One gets such wholesale returns of conjecture out of
such a trifling investment of fact.*

Mark Twain

Beschluss der Curricula-Kommission für Bachelor-, Master- und Diplomstudien vom
10.11.2008

Genehmigung des Senates am 1.12.2008

EIDESSTATTLICHE ERKLÄRUNG

Ich erkläre an Eides statt, dass ich die vorliegende Arbeit selbstständig verfasst, andere als die angegebenen Quellen/Hilfsmittel nicht benutzt, und die den benutzten Quellen wörtlich und inhaltlich entnommene Stellen als solche kenntlich gemacht habe.

Graz, am _____

Unterschrift

STATUTORY DECLARATION

I declare that I have authored this thesis independently, that I have not used other than the declared sources / resources, and that I have explicitly marked all material which has been quoted either literally or by content from the used sources.

Graz, _____

Signature

DANKSAGUNG

Allen voran möchte ich mich bei Univ.-Prof. Dr. Bernd Nidetzky für die Möglichkeit zur Durchführung der Masterarbeit am Institut für Biotechnologie und Bioprozesstechnik der TU Graz und die hervorragende und motivierende wissenschaftliche Betreuung bedanken.

Mein Dank gilt auch insbesondere meiner Arbeitsgruppe. Bei Dr. Stefan Leitgeb möchte ich mich für die weiterhelfenden fachlichen Diskussionen und den theoretischen Input bedanken. Für die Hilfestellung zur Erlernung vielerlei Arbeitstechniken für die praktische Arbeit im Labor möchte ich mich vor allem bei Mag. Thomas Stoisser sowie bei Daniela Rainer und Stephanie Gärtner, die mich auf vielerlei Weise unterstützt haben, bedanken.

Die Zeit meiner Masterarbeit wäre wohl auch ohne all die anderen hilfsbereiten MitarbeiterInnen des Institutes weitaus weniger angenehm verlaufen, so möchte ich mich für die animierende und konstruktive aber auch freundschaftliche Arbeitsatmosphäre bedanken.

Bei Dr. Ruth Birner-Grünberger möchte ich mich für die Durchführung der MALDI-TOF-MS Messungen bedanken.

Mein Dank gilt aber auch vielen hier namentlich nicht Erwähnten, meiner Familie, Freundinnen und Freunden, von denen ich Ermutigung, Kraft und Inspiration erhalten habe und die mich in der Zeit meiner Masterarbeit in mannigfacher Hinsicht motiviert und unterstützt haben. Zudem möchte ich jenen ehemaligen Lehrern danken, die mein Interesse an Naturwissenschaften erweckt und mich in mehrfacher Weise inspiriert und geprägt haben.

Abschließend möchte ich mich beim Research Center Pharmaceutical Engineering und bei Roche Diagnostics für die spannende Aufgabenstellung und die finanzielle Unterstützung bedanken.

ABSTRACT

L-Lactate oxidase (LOX) from *Aerococcus viridans* is used in biosensors to determine the level of L-lactate in blood or food. Enzyme immobilization techniques applied in biosensors can be restricted by the retention of enzymes in different matrices. In order to restrain the entrapped protein in the desired region diffusion has to be minimized which could be achieved by a size-increase of the enzyme.

Purified LOX S218C mutant was chemically modified with preferentially cysteine-directed monomethoxypoly(ethylene glycol) maleimide (mPEG-mal) with a molecular mass of 5000 Da. The covalent coupling yielded a bioconjugate with an increased mass and thereby hydrodynamic volume while the basic biological functions such as enzyme activity and stability compared to the unPEGylated native wild-type enzyme were only decreased within an acceptable range. The stability and activity of LOX were lowered due to the introduction of the mutation at Ser²¹⁸ but were not significantly further changed due to the chemical modification with the PEG chain itself.

Hence, PEGylated LOX provides an interesting approach to overcome immobilization related problems in biosensor technologies.

KURZFASSUNG

L-Laktatoxidase (*Aerococcus viridans*) wird in Biosensoren zur Bestimmung von L-Laktat im medizinischen Bereich als auch im Lebensmittelsektor eingesetzt. Die Fixierung des Enzyms in verschiedensten für die Enzymimmobilisierung eingesetzten Matrices kann dabei ein Problem darstellen. Um die Zurückhaltung des Enzyms in der gewünschten Region zu gewährleisten, müssen unerwünschte Diffusionseffekte minimiert werden. Dies könnte etwa über die Vergrößerung des Volumens des Enzyms erreicht werden.

Die L-Laktatoxidase-Mutante S218C wurde mit bevorzugt cysteingerichtetem maleimidfunktionalisierten Monomethoxypoly(ethylenglykol) (mPEG-mal) mit einem Molekulargewicht von 5000 Da chemisch verändert. Die kovalente Modifikation ergab ein Biokonjugat mit einer erhöhten Masse und somit auch einem vergrößerten hydrodynamischen Volumen. Gleichzeitig wurden die grundsätzlichen biologischen Funktionen wie Enzymaktivität und -stabilität im Vergleich zur unPEGylierten Form nur in einem akzeptablen Bereich vermindert. Bereits durch das Einführen der Mutation wurde sowohl Stabilität als auch Aktivität verringert - durch die PEGylierung selbst wurden diese allerdings nicht weiter bedeutsam beeinflusst.

Infolgedessen bereitet die PEGylierte Version der L-Laktatoxidase einen interessanten Ansatz um Probleme, die in Zusammenhang mit der Enzymimmobilisierung in Biosensortechnologien stehen, zu reduzieren bzw. zu bewältigen.

TABLE OF CONTENTS

PREFACE	1
LIST OF ABBREVIATIONS.....	2
Part A:	
TECHNICAL REPORT	5
ABSTRACT	6
REFERENCES.....	15
SUPPORTING INFORMATION	18
SUPPORTING METHODS	18
Materials	18
Molecular cloning and site-directed mutagenesis.....	18
Protein expression	19
Protein purification	20
Assays.....	20
PEGylation.....	21
Mass spectrometry	21
Spectroscopic characterization.....	22
Gel filtration analysis	22
Kinetics.....	22
Stability	23
SUPPORTING DATA.....	24
REFERENCES (SUPPORTING INFORMATION).....	25

Part B:

APPENDIX.....	27
ADDITIONAL REMARKS.....	27
S218C vs. K219C mutant	27
Attempts to improve the operational stability of LOX in biosensors	28
COMPREHENSIVELY EXPLICATED AND ADDITIONALLY USED MATERIALS AND METHODS ..	28
Materials	28
Protein expression of mutants (cultivation in flasks)	38
Protein purification	38
Enzyme assays and characterization	41
PEGylation	43
ADDITIONAL RESULTS AND DISCUSSION.....	43
Introduction of the mutations	43
Protein expression and purification.....	44
Characterization and PEGylation	45
INDICES	57
REFERENCES (APPENDIX).....	57
FIGURES	58
TABLES	60
SCHEMES.....	61

PREFACE

This master thesis is structured into two parts:

Part A is the main part of the thesis. It includes all significant results and serves as beta-version of a manuscript for a Technical Report (including Supporting Information) which is in preparation for an intended publication in Biotechnology Journal.

Part B includes additionally undertaken experiments, further aspects and more detailed descriptions of performed procedures as well as minor results obtained within these studies.

LIST OF ABBREVIATIONS

<i>A. viridans</i>	<i>Aerococcus viridans</i>
aa	amino acid
AEC	anion exchange chromatography
amp	ampicillin
Asp	aspartic acid
bp	base pairs
C, Cys	cysteine
CV	column volume
d	day(s)
dd	double distilled
dNTP	deoxyribonucleotide triphosphate
<i>E. coli</i>	<i>Escherichia coli</i>
fw	forward
h	hour(s)
HIC	hydrophobic interaction chromatography
IPTG	isopropyl β -D-1-thiogalactopyranoside
K	lysine
LB	Luria-Bertani broth
LOX	L-lactate oxidase
Lys	lysine
<i>m/z</i>	mass-to-charge-ratio
MALDI-TOF-MS	matrix-assisted laser desorption/ionization - time-of-flight - mass spectrometry
min	minute(s)
min	minute(s)
mPEG-mal 5000	methoxypoly(ethylene glycol) maleimide MW 5000 Da
mal-PEG-mal 2000	α,ω -bis-maleinimido poly(ethylene glycol) MW 2000 Da

mPEG-mal 750	methoxypoly(ethylene glycol) maleimide MW 750 Da
mPEG-mal 840	methoxypoly(ethylene glycol) maleimide MW 840 Da
MW	molecular weight
OD	optical density
on	overnight
onc	overnight culture
PPG	poly(propylene glycol)
rev	reverse
rpm	rotations per minute
s	second(s)
S, Ser	serine
SDS-PAGE	sodium dodecyl sulfate-Polyacrylamide gel electrophoresis
SEC	size exclusion chromatography
SOC	super optimal broth
T	temperature
T _m	melting temperature
V	volume
MW	molecular weight
v/v	volume per volume
w/v	weight per volume
WT	wild-type

A

TECHNICAL REPORT

Engineering of *Aerococcus viridans* L-lactate oxidase for site-specific PEGylation: characterization and chemical modification of a S218C mutant

Birgit Unterweger¹, Thomas Stoisser¹, Stefan Leitgeb¹, Ruth Birner-Grünberger², and Bernd Nidetzky^{1*}

¹ Research Center Pharmaceutical Engineering, and Institute of Biotechnology and Biochemical Engineering, Graz University of Technology, Petersgasse 12, A-8010 Graz, Austria

² Institute of Pathology and Center for Medical Research, Medical University of Graz, Stiftingtalstraße 24, A-8010 Graz, Austria

Keywords: L-Lactate oxidase; PEGylation; size-enhanced bioconjugate; biosensor; cysteine.

* Corresponding author

Telephone: +43-316-873-8400; fax: +43-316-873-8434; e-mail: bernd.nidetzky@tugraz.at

Abbreviations: AU, absorbance unit(s); FMN, flavin mononucleotide; LOX, L-lactate oxidase; mAU, milli-absorbance unit(s); mPEG, methoxypoly(ethylene glycol); mPEG-mal 5000, monomethoxypoly(ethylene glycol) maleimide 5000; PEG, poly(ethylene glycol); PDB, Protein Data Bank; TOF, time-of-flight; v, volume; w, weight; WT, wild-type.

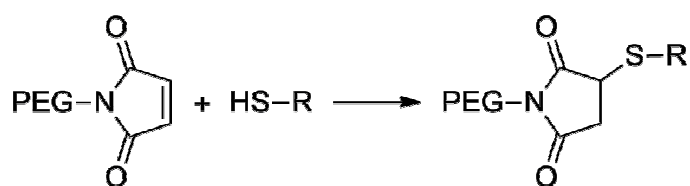
ABSTRACT

Aerococcus viridans L-lactate oxidase (LOX) is widely used in the clinical analysis of L-lactate. Immobilization of LOX in analytical devices is usually done through a combination of adsorption and entrapment. Considering the possible benefit of enzyme size enhancement for the LOX immobilization, we have designed a substantially enlarged bioconjugate of the enzyme that harbors site-directed replacement of Ser²¹⁸ by Cys and is derived from Cys-directed modification of the mutated LOX with maleimide-activated methoxypoly(ethylene glycol) (mPEG) 5000. The mutated LOX and the mPEGylated derivative thereof retained activity and stability within an order of magnitude of the corresponding levels for the wild-type enzyme. The substrate specificity of LOX was not changed as result of the mutation or the derivatization of the mutant with mPEG 5000.

L-Lactate oxidase (EC 1.13.12.4; LOX) is a long-known and well-studied flavin mononucleotide (FMN)-dependent enzyme that catalyzes oxidation of L-lactate into pyruvate [1]. O₂ serves as the terminal electron acceptor of the enzymatic reaction that gives H₂O₂ as its second product. Even though LOX is absolutely S-enantioselective, the enzyme has a relatively broad specificity for the α-hydroxy acid substrate used [2, 3, 4]. Application of LOX in the biocatalytic resolution of chemicals bearing a racemic α-hydroxy acid functional group has therefore attracted some attention [5, 6]. However, LOX has its major uses in medical analytics where the enzyme is applied widely as biological transducer of different biosensors and test strips [7, 8, 9, 10, 11]. LOX from the bacterium *Aerococcus viridans* has been well characterized biochemically, and a high-resolution crystal structure has been determined for this homotetrameric enzyme [12, 13, 14, 15].

The enzymatically active part of the analytical device is usually a thin solid film in which the used LOX is immobilized through the combined physical effects of adsorption to and entrapment within the matrix materials [16, 17, 18, 19, 20, 21]. In the absence of covalent fixation, strength of retention of the enzyme in the matrix can be a problem. Even though chemical crosslinking with a bifunctional reagent such as glutardialdehyde presents a possible solution, there are the clear disadvantages that the crosslinking very often results in large losses of the enzyme activity and homogeneous distribution of the crosslinked, sometimes partly insoluble enzyme in the matrix can become a serious issue [22, 23]. A method providing controlled size enhancement for the soluble LOX would facilitate stable embedment of the enzyme in the sensor matrix, and it should additionally be compatible with the currently used immobilization procedures.

A novel concept of bioconjugation by design is proposed for LOX that exploits cysteine-directed chemical modification of the protein with PEG (Scheme 1) [24].



(1)

Scheme 1: Reaction of maleimide-activated PEG with the side chain of cysteine.

The LOX from *A. viridans* which does not contain cysteines in its wild-type form was mutated at position 218 (Figure 1) where a seemingly well accessible Ser is positioned on the surface of the structure of the native protein. Moreover, the site for covalent attachment of a PEG molecule was considered to be sufficiently far away from the enzyme active site to prevent interference with LOX function after derivatization of Cys²¹⁸.

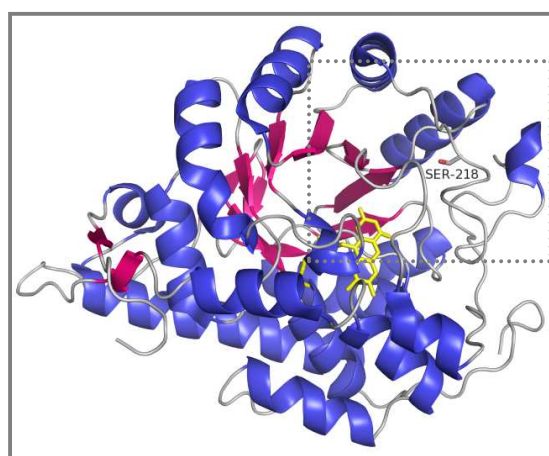
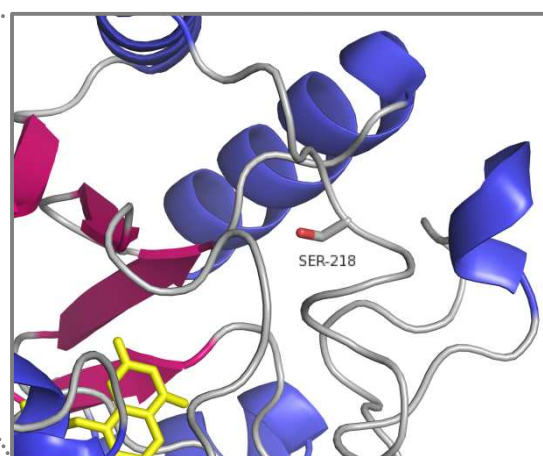
1A**1B**

Figure 1: Overall fold of the subunit of *A. viridans* LOX (1A) and close up of the protein site used for introduction of a cysteine (1B); (PDB accession number: 2DU2).

The resulting S218C mutant was obtained by expression in *E. coli*, and we show successful modification of the isolated mutant with maleimide-activated methoxypoly(ethylene glycol) (mPEG) 5000.

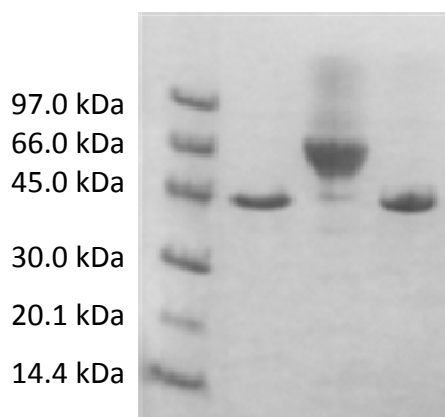
Mutations in the native LOX gene (accession number: D50611.1) resulting in site-directed substitution of Ser²¹⁸ by Cys were introduced by a two-stage PCR employing suitable oligonucleotide primers [25]. The mutated gene was verified by sequencing and placed into plasmid vector pLO-1 that provided target gene expression under control of the *tac* promoter. Enzyme production was done in *E. coli* BL21 (DE3) using controlled cultivation conditions in a 5-L stirred bioreactor. The S218C mutant was obtained in apparent electrophoretic homogeneity (Figure 2A) by using a two-step purification consisting of ammonium sulfate precipitation of non-LOX protein from *E. coli* cell extract followed by

hydrophobic interaction chromatography. The Supporting Information gives full details on the methods used for generation, expression and purification of the S218C mutant.

The mutated LOX was recovered in a yield of 27% and its specific activity measured with a standard peroxidase-coupled assay (Sigma) using 50 mM L-lactate as substrate (37 °C, pH 6.5) was 90 U/mg [26]. By way of comparison, the specific activity of wild-type LOX produced and purified in exactly the same way as the mutant was about 200 U/mg. The commercial preparation of the wild-type enzyme (Roche Diagnostics) displayed identical specific activity. Additionally, it appeared to be essentially pure by the criterion of migration as single protein band in SDS-PAGE, as shown in the Supporting Information. Therefore and because of convenient availability, we used the commercial LOX as reference for the characterization of the S218C mutant.

Figure 2B shows an overlay of the visible absorbance spectra of S218C mutant and wild-type LOX, both recorded at an exactly comparable protein concentration. Each spectrum contains two prominent bands with wavelengths of maximum absorption at around 375 nm and 455 nm that are highly characteristic of the FMN cofactor in its oxidized form [27]. The spectrum of the mutant was nearly superimposable on the reference spectrum, suggesting that binding of FMN to LOX was essentially unaffected by the site-directed substitution of Ser²¹⁸. The result also implies that catalytic constants for the two enzymes can be compared with the assumption of a similar occupancy of their respective FMN binding site. The saturation of the protein with the prosthetic group can be calculated as about 50% assuming a molar extinction coefficient of 12500 M⁻¹ cm⁻¹ at 445 nm as known for free FMN [28].

2A



2B

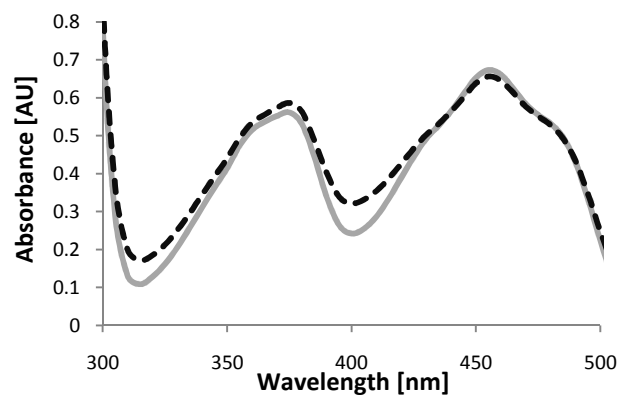


Figure 2: PEGylation of purified S218C mutant monitored by SDS-PAGE (2A) and comparison of the visible absorbance spectrum of the mutated LOX with that of the wild-type enzyme (2B). 2A: lane 1, molecular mass markers; lane 2, unPEGylated WT; lane 3, PEGylated S218C; lane 4, WT LOX undergone identical PEGylation conditions; 2B: WT (broken black line) and S218C (full light gray line) absorbance spectra showing the characteristic peaks of FMN in its oxidized form were recorded at a protein concentration of 0.1 mM enzyme in 50 mM potassium phosphate buffer, pH 7.0 at 25 °C.

For PEGylation, the purified S218C mutant (8 μ M) was incubated in 50 mM potassium phosphate buffer, pH 7.0, at 4 °C. Monomethoxypoly(ethylene glycol) maleimide 5000 (mPEG-mal 5000; Sigma-Aldrich) was added, and incubation was performed under gentle agitation (300 rpm; Eppendorf Thermomixer) [29]. Different molar ratios of enzyme and mPEG-mal 5000 were tested and a 12.5-fold molar surplus of mPEG-mal 5000 was found to give exhaustive modification of the protein. After 4 h of reaction, which was sufficient for the reaction to go to completion (data not shown), excess of mPEG-mal 5000 was removed by repeated ultrafiltration with Vivaspin 6 centrifugal concentrator tubes. PEGylated S218C mutant was used immediately for further characterization. The wild-type enzyme was treated in exactly the same manner.

We used SDS-PAGE for detection of protein modification by mPEG-mal 5000. Figure 2A shows that the apparent molecular mass of wild-type LOX had not been affected by incubation with mPEG-mal 5000, suggesting the absence of PEGylation, as expected. The S218C mutant by contrast displayed a clear shift in apparent mass to a higher value due to the PEGylation reaction, indicating that derivatization of the mutated LOX had taken place.

The absence of a protein band corresponding to the unmodified mutant in the sample analyzed implies that the chemical modification of the S218C mutant had been complete under the conditions used. MS analysis of the S218C mutant prior to and after incubation with mPEG-mal 5000 gave more detailed information about the process of PEGylation. Figure 3 shows that the underivatized enzyme, which displayed the expected molecular mass of 41 kDa, had disappeared entirely from the protein sample after the PEGylation reaction, corroborating the results of SDS-PAGE (Figure 2A). Two new macromolecular species were formed in the reaction, and they were present in different amounts. The by far abundant species displayed a mass of 46 kDa, consistent with the idea that the unmodified S218C mutant had acquired the extra mass of +5 kDa resulting from attachment of one mPEG-mal 5000 to the protein, presumably to Cys²¹⁸. The second mass peak of 51 kDa could have originated from a double modification of the mutant. The site(s) of modification of the S218C mutant with mPEG-mal 5000 were not identified in the MS analysis. However, aggregate data on the chemical modification of the S218C mutant (Figures 2A and 3) plus the absence detectable modification in the wild-type enzyme strongly suggest Cys²¹⁸ as the major site of derivatization by mPEG-mal 5000.

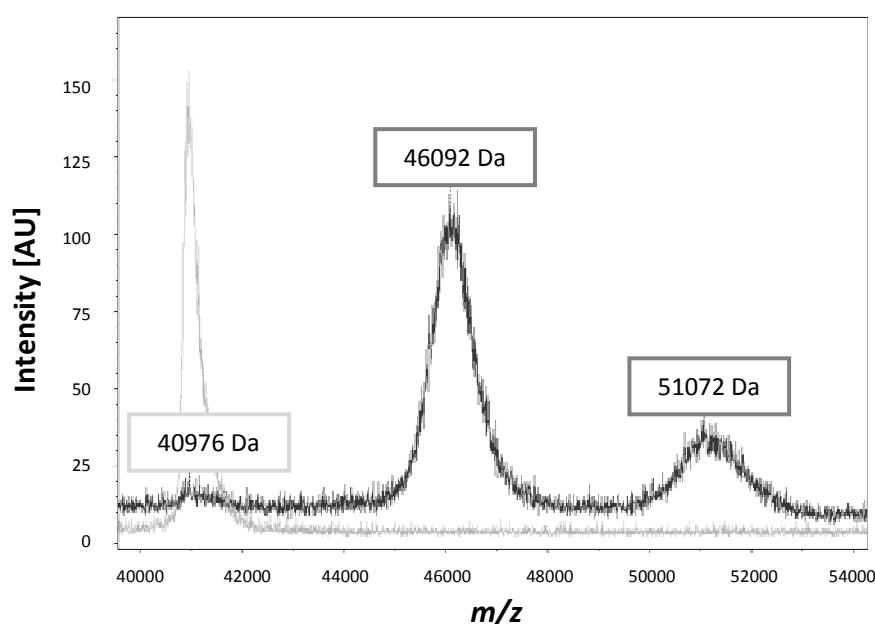


Figure 3: PEGylation of S218C mutant monitored by MS. Peaks at 41 kDa, 46 kDa and 51 kDa, respectively, represent unPEGylated (light gray line), monoPEGylated and doublePEGylated (dark gray line) S218C forms. Details of MALDI-TOF-MS analysis are given in Supporting Information.

To examine enlargement of the hydrodynamic volume of the S218C mutant resulting from PEGylation, we performed gel filtration analysis using conditions in which direct interaction of protein and PEG with the chromatographic material should have been minimized. The elution profiles of the PEGylated and underivatized forms of the mutant are superimposed in Figure 4. The results are clear in showing a marked size enhancement for the PEGylated enzyme, whose elution volume corresponded to an apparent molecular mass of approximately 250 kDa.

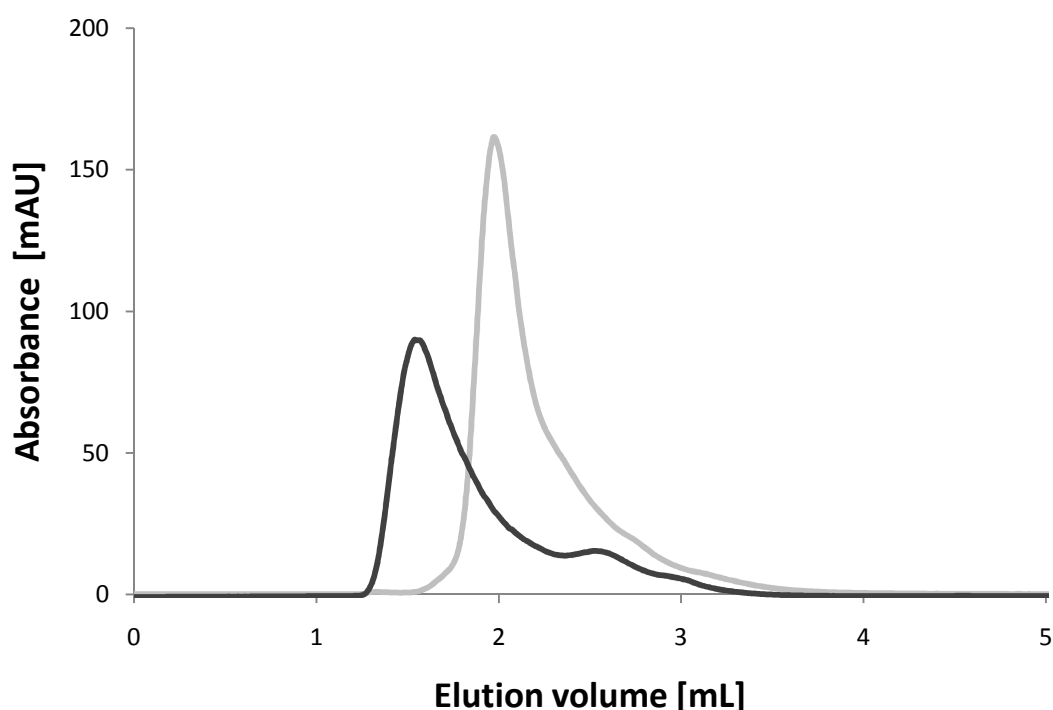


Figure 4: Gel filtration analysis for S218C mutant and the PEGylated derivative thereof. 50 μ L of 3 mg/mL solutions of PEGylated (full dark gray line) and unPEGylated (full light gray line) LOX S218 mutant, respectively, were loaded on a Superdex 200 column (GE Healthcare Life Sciences) and eluted isocratically at 25 $^{\circ}$ C with 50 mM potassium phosphate buffer containing 150 mM NaCl, pH 7.0 with a flow rate of 0.5 mL/min and detection at 280 nm.

To obtain more detailed information about functional consequences of the site-directed replacement of Ser²¹⁸ by Cys and of the modification by mPEG-mal 5000, we carried out a steady-state kinetic characterization of the S218C mutant both in unmodified and PEGylated form. Table 1 summarizes the results, showing kinetic parameters for the two preparations of the mutant along with kinetic parameters for the wild-type enzyme. The mutation

resulted in a 2.7-fold loss in catalytic efficiency for reaction with L-lactate (k_{cat}/K_M). This loss can be ascribed almost exclusively to a decrease in turnover number (k_{cat}) caused by the mutation. Apparent substrate binding (K_M) was hardly affected in the mutant. When compared to its unmodified counterpart, the PEGylated mutant displayed a slight loss in k_{cat}/K_M , again resulting from a corresponding decrease in k_{cat} . The PEGylated mutant was about one-fourth as efficient as the wild-type enzyme.

Table 1: Kinetic characterization of PEGylated and unmodified forms of S218C for reaction with L-(+)-Lactic acid.

Mutant	Specific activity [U/mg]	k_{cat} [s^{-1}]	K_M [mM]	k_{cat}/K_M [[$\text{s} \cdot \text{mM}$] $^{-1}$]
WT	204	140	0.83	167
S218C	90	62	1.0	61
PEGylated S218C	62	43	1.0	42

We further tested a series of α -hydroxy acids that serve as alternative substrates of the wild-type enzyme. Table S3 in Supporting Information shows the results, indicating that the overall substrate specificity of LOX has not been changed as result of mutation and PEGylation.

We finally examined the stability of the S218C mutant, unmodified and PEGylated, measuring irreversible loss of activity during incubation at 37 °C. Figure 5 shows that the unmodified mutant was inactivated somewhat faster than the wild-type enzyme, showing a decrease in half-life time by a factor of about 2.5. The stability of the mutant was unchanged after the PEGylation.

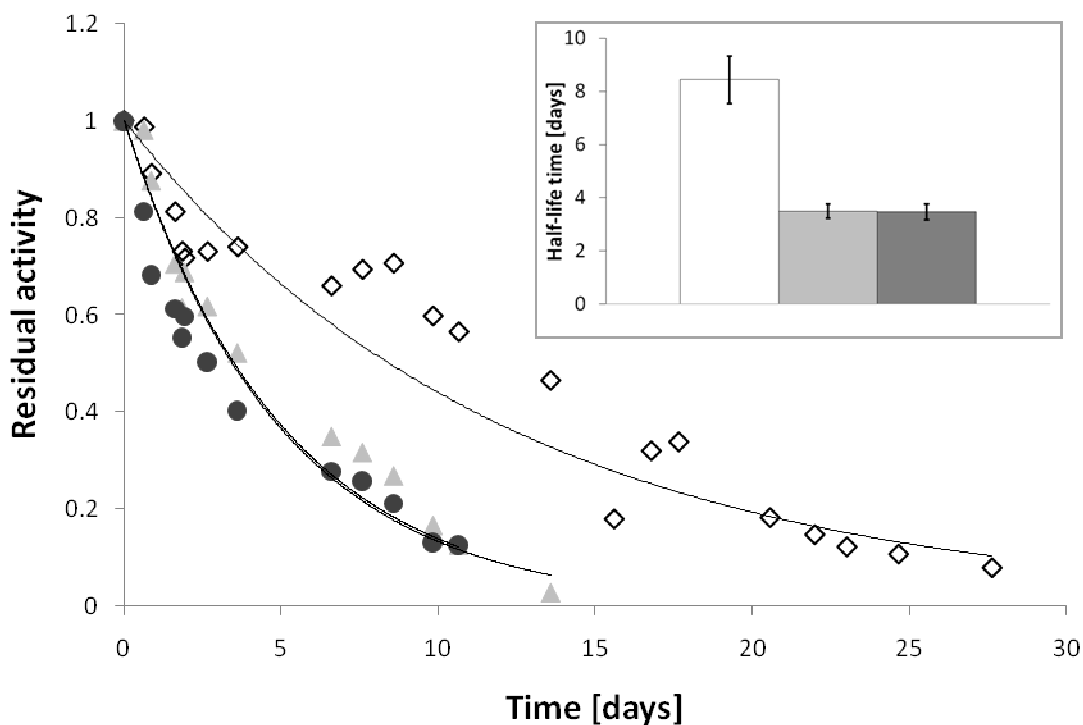


Figure 5: Inactivation time courses for S218C mutant (light gray triangles) and the PEGylated derivative (dark gray circles) thereof in comparison to wild-type LOX (white diamonds). Residual activity is expressed as fraction of the starting activity. The inset shows half-life times calculated from the data assuming pseudo-first order decay of activity. Stability of WT (white bar), S218C (light gray bar) and PEGylated S218C (dark gray bar) were determined by measuring the residual activity when incubated in 40 mM HEPES containing 150 mM NaCl, pH 8.1 at 37 °C.

In conclusion, we have achieved the intended substantial size enhancement of LOX using a new bioconjugation approach in solution that was based on introduction of a single Cys at position 218, identified through structure-guided selection, and Cys-directed modification with mPEG-mal 5000. Marked loss of activity and/or stability is a problem often encountered in the preparation of enzyme bioconjugates. Even though replacement of Ser²¹⁸ of Cys was not silent, with regard to decreasing catalytic efficiency and resistance to inactivation at 37 °C, as it was striven for, the S218C mutant could still be considered a quite useful catalyst. Importantly, the final PEGylation left the properties of the mutated enzyme unaffected and proceeded with excellent yield of modification.

REFERENCES

- [1] Maeda-Yorita, K., Aki, K., Sagai, H., Misaki H. and Massey, V., L-lactate oxidase and L-lactate monooxygenase: mechanistic variations on a common structural theme. *Biochimie*. 1995, 77, 631-642.
- [2] Umena, Y., Yorita, K., Matsuoka, T., Kita, A., Fukui K. and Morimoto, Y., The crystal structure of L-lactate oxidase from *Aerococcus viridans* at 2.1Å resolution reveals the mechanism of strict substrate recognition. *Biochem. Biophys. Res. Commun.* 2006, 350, 249-256.
- [3] Yorita, K., Aki, K., Ohkuma-Soyejima, T., Kokubo, T., Misaki, H. and Massey, V., Conversion of L-lactate oxidase to a long chain alpha-hydroxyacid oxidase by site-directed mutagenesis of alanine 95 to glycine. *J. Biol. Chem.* 1996, 271, 28300-28305.
- [4] Yorita, K., Janko, K., Aki, K., Ghisla, S., Palfey, B. A. and Massey, V., On the reaction mechanism of L-lactate oxidase: quantitative structure-activity analysis of the reaction with para-substituted L-mandelates. *Proc. Natl. Acad. Sci. USA.* 1997, 94, 9590-9595.
- [5] Oikawa, T., Mukoyama, S. and Soda, K., Chemo-enzymatic D-enantiomerization of DL-lactate. *Biotechnol. Bioeng.* 2001, 73, 80-82.
- [6] Soda, K., Oikawa, T. and Yokoigawa, K., One-pot chemo-enzymatic enantiomerization of racemates. *J. Mol. Catal. B Enzym.* 2001, 11, 149-153.
- [7] Mehrvar, M. and Abdi, M., Recent developments, characteristics, and potential applications of electrochemical biosensors. *Anal. Sci.* 2004, 20, 1113-1126.
- [8] Minagawa, H., Nakayama, N., Matsumoto, T. and Ito, N., Development of long life lactate sensor using thermostable mutant lactate oxidase. *Biosens. Bioelectron.* 1998, 13, 313-318.
- [9] Wang, J. and Chen, Q., Enzyme microelectrode array strips for glucose and lactate. *Anal. Chem.* 1994, 66, 1007-1011.
- [10] Romero, M. R., Ahumada, F., Garay, F. and Baruzzi, A. M., Amperometric biosensor for direct blood lactate detection. *Anal. Chem.* 2010, 82, 5568-5572.
- [11] Schuvailo, O. M., Soldatkin, O. O., Lefebvre, A., Cespuglio, R. and Soldatkin, A. P., Highly selective microbiosensors for in vivo measurement of glucose, lactate and glutamate. *Anal. Chim. Acta.* 2006, 573-574, 110-116.

- [12] Furuichi, M., Suzuki, N., Dhakshnamoorthy, B., Minagawa, H., Yamagishi, R., Watanabe, Y., Goto, Y., Kaneko, H., Yoshida, Y., Yagi, H., Waga, I., Kumar, P. K. and Mizuno, H., X-ray structures of *Aerococcus viridans* lactate oxidase and its complex with D-Lactate at pH 4.5 show an α -hydroxyacid oxidation mechanism. *J. Mol. Biol.* 2008, 378, 436-446.
- [13] Li, S. J., Umena, Y., Yorita, K., Matsuoka, T., Kita, A., Fukui, K. and Morimoto, Y., Crystallographic study on the interaction of L-lactate oxidase with pyruvate at 1.9 Å resolution. *Biochem. Biophys. Res. Commun.* 2007, 358, 1002-1007.
- [14] Leiros, I., Wang, E., Rasmussen, T., Oksanen, E., Repo, H., Petersen, S. B., Heikinheimo, P. and Hough, E., The 2.1 Å structure of *Aerococcus viridans* L-lactate oxidase (LOX). *Acta Crystallogr. Sect. F Struct. Biol. Cryst. Commun.* 2006, 62, 1185-1190.
- [15] Yorita, K., Matsuoka, T., Misaki, H. and Massey, V., Interaction of two arginine residues in lactate oxidase with the enzyme flavin: conversion of FMN to 8-formyl-FMN. *Proc. Natl. Acad. Sci. USA.* 2000, 97, 13039-13044.
- [16] Patel, N. G., Erlenkötter, A., Cammann, K. and Chemnitz, G.-C., Fabrication and characterization of disposable type lactate oxidase sensors for dairy products and clinical analysis. *Sens. Actuators B Chem.* 2000, 67, 134-141.
- [17] Zanina, V. P., López de Mishimaa, B. and Solís, V., An amperometric biosensor based on lactate oxidase immobilized in laponite-chitosan hydrogel on a glassy carbon electrode. Application to the analysis of L-lactate in food samples. *Sens. Actuators B Chem.* 2010, 155, 75-80.
- [18] Huang, J., Li, J., Yang, Y., Wang, X., Wu, B., Anzai, J.-i., Osa, T. and Chen, Q., Development of an amperometric L-lactate biosensor based on L-lactate oxidase immobilized through silica sol-gel film on multi-walled carbon nanotubes/platinum nanoparticle modified glassy carbon electrode. *Mater. Sci. Eng. C.* 2008, 28, 1070-1075.
- [19] Mueller, A., Enzyme electrodes for medical sensors. *Mini Rev. Med. Chem.* 2005, 5, 231-239.
- [20] Park, B. W., Yoon, D. Y. and Kim, D. S., Recent progress in bio-sensing techniques with encapsulated enzymes. *Biosens. Bioelectron.* 2010, 26, 1-10.
- [21] Schaffar, B. P. H., F. Hoffmann La Roche AG. *Creatinine biosensor. PCT Int. Appl.* 2001, WO 01/87300 A1.

- [22] Romero, M. R., Garay, F. and Baruzzi, A. M., Design and optimization of a lactate amperometric biosensor based on lactate oxidase cross-linked with polymeric matrixes. *Sens. Actuators. B Chem.* 2008, *131*, 590-595.
- [23] Migneault, I., Dartiguenave, C., Bertrand, M. J. and Waldron, K. C., Glutaraldehyde: behavior in aqueous solution, reaction with proteins, and application to enzyme crosslinking. *Biotechniques.* 2004, *37*, 790-802.
- [24] Veronese, F. M., Peptide and protein PEGylation: a review of problems and solutions. *Biomaterials.* 2001, *22*, 405-417.
- [25] Wang, W. and Malcom, B. A., Two-stage PCR protocol allowing introduction of multiple mutations, deletions and insertions using QuikChange Site-Directed Mutagenesis. *Biotechniques.* 1999, *26*, 680-682.
- [26] Lockridge, O., Massey, V. and Sullivan, P. A., Mechanism of action of the flavoenzyme lactate oxidase. *J. Biol. Chem.* 1972, *247*, 8097-8106.
- [27] Macheroux, P., UV-visible spectroscopy as a tool to study flavoproteins. in: Chapman, S.K. and Reid, G. A. (Eds.), *Methods Mol. Biol., vol. 131: Flavoprotein Protocols.* Humana Press Inc., Totowa, NJ 1999, pp. 1-7.
- [28] Munro, A. W. and Noble, M. A., Fluorescence analysis of flavoproteins. in: Chapman, S.K. and Reid, G. A. (Eds.), *Methods Mol. Biol., vol. 131: Flavoprotein Protocols.* Humana Press Inc., Totowa, NJ 1999, pp. 25-48.
- [29] Slavica, A., Dib, I. and Nidetzky, B., Selective modification of surface-exposed thiol groups in *Trigonopsis variabilis* D-amino acid oxidase using poly(ethylene glycol) maleimide and its effect on activity and stability of the enzyme. *Biotechnol. Bioeng.* 2007, *96*, 9-17.

SUPPORTING INFORMATION

SUPPORTING METHODS

Materials

Monomethoxypoly(ethylene glycol) maleimide (mPEG-mal) 5000, L-(+)-lactic acid, (S)-2-hydroxybutyric acid and (S)-2-hydroxyisocaproic acid in the highest available purity, 3,3-dimethylglutaric acid, 4-aminoantipyrine, peroxidase from horseradish, N,N-dimethylaniline and dodecylbenzenesulfonic acid were obtained from Sigma-Aldrich or Fluka. Lyophilized native L-lactate oxidase wild-type (WT) serving as reference and the plasmid pLO-1 carrying the genetic information for the WT L-lactate oxidase (LOX) were kindly provided by Roche Diagnostics and stored at -25 °C until further use.

Molecular cloning and site-directed mutagenesis

Table S1: Used oligonucleotides for site-directed mutagenesis.

Primername	Sequence	T _m [°C]
S218Cfw	5'-GGTGCTT <u>G</u> CAAACAAAAAATCTACCAAGAGATATTG-3'	61.3
S218Crev	5'-TTGTTT <u>G</u> CAAGCACCGTAGATATTGTTTAATGACATACC-3'	61.4

The mutation S218C was introduced into LOX using a reported two-stage PCR protocol [S1]. Briefly, two separate primer extension reactions containing pLO-1 as template and the respective mutagenic primer (listed in Table S1), forward or reverse, were set-up. DNA was amplified by Pfu DNA Polymerase from Promega in the corresponding buffer in the presence of dNTPs under the following conditions: After heat denaturation at 95 °C for 1 min, 4 treatment cycles, each consisting of 95 °C for 50 s, 59 °C for 50 s and 68 °C for 10 min, were applied, followed by 68 °C for 7 min and cooling at 4 °C. The two separate reactions were combined in the ratio 1:1 and the PCR was performed as described above, but with a total

repeat of 18 cycles. Template DNA was digested with *DpnI* at 37 °C for 1 h. Plasmid DNA was transformed into electrocompetent *E. coli* BL21 (DE3) cells. After regeneration in SOC medium the cells were cultured overnight at 37 °C on LB-amp plates (1% peptone, 0.5% yeast extract, 0.5% NaCl, 1.8% agar supplemented with 100 µg/mL ampicillin). Only transformants carrying plasmids with the mutation of interest verified by DNA sequencing were used for further steps.

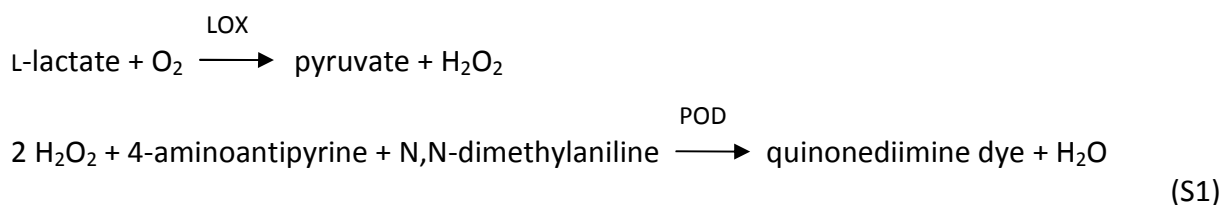
Protein expression

E. coli BL21 (DE3) cells harboring the plasmid containing the S218C mutant gene were grown overnight as starter culture (0.55% glucose monohydrate, 1% peptone, 0.5% yeast extract, 0.5% NaCl, 0.1% NH₄Cl, 0.025% MgSO₄*H₂O, 100 µL/L poly(propylene glycol), 0.3% K₂HPO₄, 0.6% KH₂PO₄, 0.2*10⁻³% thiamine, 11.5*10⁻³% ampicillin, 0.4*10⁻³% FeSO₄*7 H₂O, 0.1*10⁻³% MnSO₄*H₂O, 0.04*10⁻³% CoCl₂, 0.015*10⁻³% CuSO₄*5 H₂O, 0.01*10⁻³% H₃BO₃, 0.02*10⁻³% ZnSO₄*7 H₂O, 0.02*10⁻³% Na₂MoO₄*2 H₂O and 0.04*10⁻³% FeCl₃). The main culture (same medium as for the starter culture except of a 4-fold higher amount of glucose monohydrate) was inoculated to an OD₆₀₀ of 0.5. Temperature, stirring, pH and oxygen partial pressure in the B. Braun Biotech International Biostat®C, Type CT5-2 fermenter were controlled and adjusted automatically. The pH was balanced at pH 7.0 with 2 M KOH and 1 M H₃PO₄, the pO₂ was fixed to a minimum of 40%. The cells were grown at 37 °C before induction. At an OD₆₀₀ of about 2 isopropyl β-D-1-thiogalactopyranoside was added to a final concentration of 0.25 mM. Simultaneously the medium was supplemented with 115 mg/L ampicillin. Upon induction the cells were cultured at 30 °C. When the level of glucose was lower than 1 mg/mL (Diabur Test 5000, Roche Diagnostics) cells were harvested. The pellet was suspended in 50 mM potassium phosphate buffer, pH 7.0 and stored at -25 °C.

Protein purification

Cells were disrupted by French pressing. The crude extract was obtained via centrifugation. After precipitation in the presence of 1.5 M $(\text{NH}_4)_2\text{SO}_4$ at 4 °C and the removal of the precipitate by centrifugation, the L-lactate oxidase was purified by hydrophobic interaction chromatography using a Phenyl Sepharose 6 Fast Flow (High Sub) column (GE Healthcare Life Sciences) and an Äkta FPLC system (Amersham Biosciences). The protein was loaded on the column equilibrated with 50 mM potassium phosphate buffer, pH 7.0 and eluted at 25 °C with a linear increasing salt concentration with 50 mM potassium phosphate buffer containing 1.5 M ammonium sulfate, pH 7.0 with a flow rate of lower than 6 mL/min and detection at 280 nm. Fractions containing significant amounts of active protein as determined with the below described spectrophotometric stop rate determination were pooled and the purity was verified by SDS-PAGE, using PhastGel™ Gradient 8-25 (GE Healthcare Life Sciences) gels and the Pharmacia High Speed Electrophoresis System (Pharmacia Biotech). S218C LOX solution was then desalted by repeated cycles of concentration and dilution using ultrafiltration devices (Vivaspin 20, 10 kDa cutoff, Vivascience AG, Hannover, Germany) and stored in 50 mM potassium phosphate buffer at -25 °C until further use.

Assays



Scheme S1: Activity assay.

The activity was determined using a reported standard peroxidase-coupled spectrophotometric assay (Sigma) [S2]. 5-10 μL of LOX enzyme version appropriately diluted in 50 mM potassium phosphate buffer was added to an activity assay containing

40 mM 3,3-dimethylglutaric acid, 2.5 units peroxidase, 1.5 mM 4-aminoantipyrine, 50 mM L-(+)-lactic acid and 0.04% (volume/volume; v/v) N,N-dimethylaniline in a total volume of 0.5 mL reaction mixture at pH 6.5. After a reaction time of 10-20 min at 37 °C 1 ml 0.25% (weight/volume; w/v) dodecylbenzenesulfonic acid solution was then added to stop the reaction. The produced quinonediimine dye was measured spectrophotometrically at 565 nm with a Varian Cary® 50 Bio UV-Visible Spectrophotometer at 25 °C.

Protein concentrations were measured according to the Bradford protein quantification assay (Roti®-Quant, Carl Roth GmbH + Co KG) using BSA as reference.

PEGylation

PEGylation was achieved in similarity to a procedure reported elsewhere [S3]. Briefly, the purified S218C mutant (8 µM) was incubated in the presence of a 12.5-fold molar excess of monomethoxypoly(ethylene glycol) maleimide 5000 (mPEG-mal 5000; Sigma-Aldrich) in 50 mM potassium phosphate buffer, pH 7.0, at 4 °C for 4 h under gentle agitation (300 rpm; Eppendorf Thermomixer). To remove residual mPEG-mal 5000 repeated ultrafiltration with Vivaspin 6 centrifugal concentrator tubes (10 kDa cutoff, Vivascience AG, Hannover, Germany) was performed. PEGylated S218C mutant was used immediately for further characterization.

Mass spectrometry

For MALDI-TOF (time-of-flight)-MS measurement on a Bruker Ultraflex extreme instrument, protein solutions (2.4 mg/mL (PEGylated) or 7.2 mg/mL (unPEGylated) in 50 mM potassium phosphate buffer, pH 7.0) were diluted in 50% acetonitrile and 0.1% trifluoroacetic acid 1:5 (v/v) and mixed 1:1 (v/v) with a suspension of 5 mg super-DHB matrix (Sigma, 9:1 mixture of 2,5-dihydroxybenzoic acid and 2-hydroxy-5-methoxybenzoic acid) in 50 µL acetonitrile and 50 µL 0.1% trifluoroacetic acid. 1 µL was spotted onto an

800 μm Bruker MTP Anchorchip and left to dry. Full MS spectra were obtained in positive linear mode after external calibration using an appropriate protein standard (10-70 kDa) in the mass/charge range from 550 to 73000 by summarising 9000 laser shots.

Spectroscopic characterization

UV-visible absorbance spectra showing the characteristic absorption maxima of the FMN-peaks were recorded with a Varian Cary® 50 Bio UV-Visible Spectrophotometer in quartz cuvettes (Hellma® GmbH & Co. KG) of 10 mm light path. 0.1 mM enzyme in potassium phosphate buffer, pH 7.0 was scanned at 25 °C and the values corrected for blank readings.

Gel filtration analysis

Gel filtration analysis was undertaken using a Superdex 200 column (GE Healthcare Life Sciences) and an Äkta FPLC system (Amersham Biosciences). 50 μL of 3 mg/mL solutions of the respective protein version were loaded on the column. Isocratic elution was performed with 50 mM potassium phosphate buffer containing 150 mM NaCl, pH 7.0 at 25 °C with a flow rate of 0.5 mL/min and detection at 280 nm.

Kinetics

To determine kinetic characteristics for L-(+)-lactic acid and alternative substrates at pH 6.5, the substrate concentration was varied over a significant range (10 suitable concentrations within 50 mM to 0.1 mM) and the peroxidase-coupled spectrophotometric assay was performed as described above. K_M - and v_{max} -values were obtained by a nonlinear fit of the Michaelis-Menten equation to the measured data with Sigma Plot®. K_{cat} -values were calculated on the basis of protein concentrations.

Stability

To determine the irreversible enzyme inactivation 0.2-0.4 μM (corresponding to similar starting activities of WT, S218C and PEGylated S218C) of the respective protein preparation were incubated in 40 mM HEPES buffer containing 150 mM NaCl, pH 8.1 at 37 °C (Eppendorf Thermomixer). Samples were taken at different time-points and then the residual enzyme activity was determined with the above described activity measurement. The half-life times of the different enzyme preparations were determined by an exponential curve fit to the obtained data assuming pseudo-first order decay of activity.

SUPPORTING DATA

Table S2: Purification of S218C mutant.

Purification step	Specific activity [U/mg]	Recovery rate [%U]
Crude extract	15	100
(NH ₄) ₂ SO ₄ precipitation	24	89
HIC pool a	56	8
HIC pool b after desalting	90	27

Table S3: Substrate specificities of different LOX forms.

Mutant	Substrate	Specific activity [U/mg]	k_{cat} [s ⁻¹]	K_M [mM]	k_{cat}/K_M [(s*mM) ⁻¹]
WT	(S)-2-Hydroxybutyric acid	2.0	1.4	0.43	3.2
S218C		2.5	1.8	4.0	0.45
PEGylated S218C		2.4	1.7	4.1	0.41
WT	(S)-2-Hydroxyisocaproic acid	1.6	1.1	0.43	2.5
S218C		0.4	0.27	0.26	1.1
PEGylated S218C		0.5	0.35	0.82	0.4

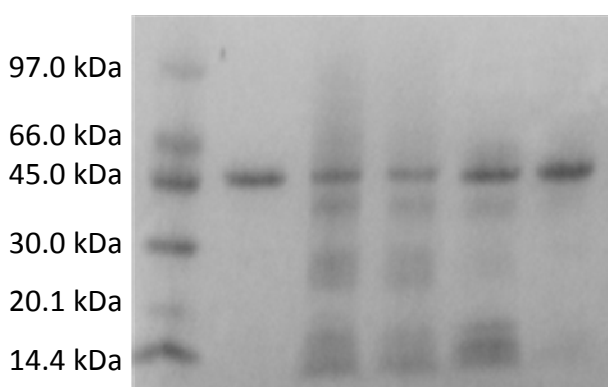


Figure S1: Purification of S218C mutant documented by SDS-PAGE; lane 1, molecular mass marker; lane 2, WT LOX; lane 3, S218C LOX crude extract; lane 4, S218C LOX after (NH₄)₂SO₄ precipitation; lane 5 and 6, S218C LOX pool a and b after HIC purification.

REFERENCES (SUPPORTING INFORMATION)

[S1] Wang, W. and Malcom, B. A., Two-stage PCR protocol allowing introduction of multiple mutations, deletions and insertions using QuikChange Site-Directed Mutagenesis. *Biotechniques*. 1999, 26, 680-682.

[S2] Lockridge, O., Massey, V. and Sullivan, P. A., Mechanism of action of the flavoenzyme lactate oxidase. *J. Biol. Chem.* 1972, 247, 8097-8106.

[S3] Slavica, A., Dib, I. and Nidetzky, B., Selective modification of surface-exposed thiol groups in *Trigonopsis variabilis* D-amino acid oxidase using poly(ethylene glycol) maleimide and its effect on activity and stability of the enzyme. *Biotechnol. Bioeng.* 2007, 96, 9-17.

B

APPENDIX

ADDITIONAL REMARKS

In this section additionally done work and further aspects are discussed.

S218C vs. K219C mutant

Besides the S218C mutant of LOX discussed in the main part of this thesis also K219C was created following the same mutagenesis strategy as described above. Ser²¹⁸ and Lys²¹⁹ are both located on the protein surface as shown in Figure 6. While Ser²¹⁸ is only included in a weak interaction (3.51 Å), Lys²¹⁹ interacts with an aspartic acid residue of a nearby α -helix (2.83 Å). This implies that the mutation at this site might result in a structural change of LOX and thus changes the enzyme functions in an unfavorable manner.

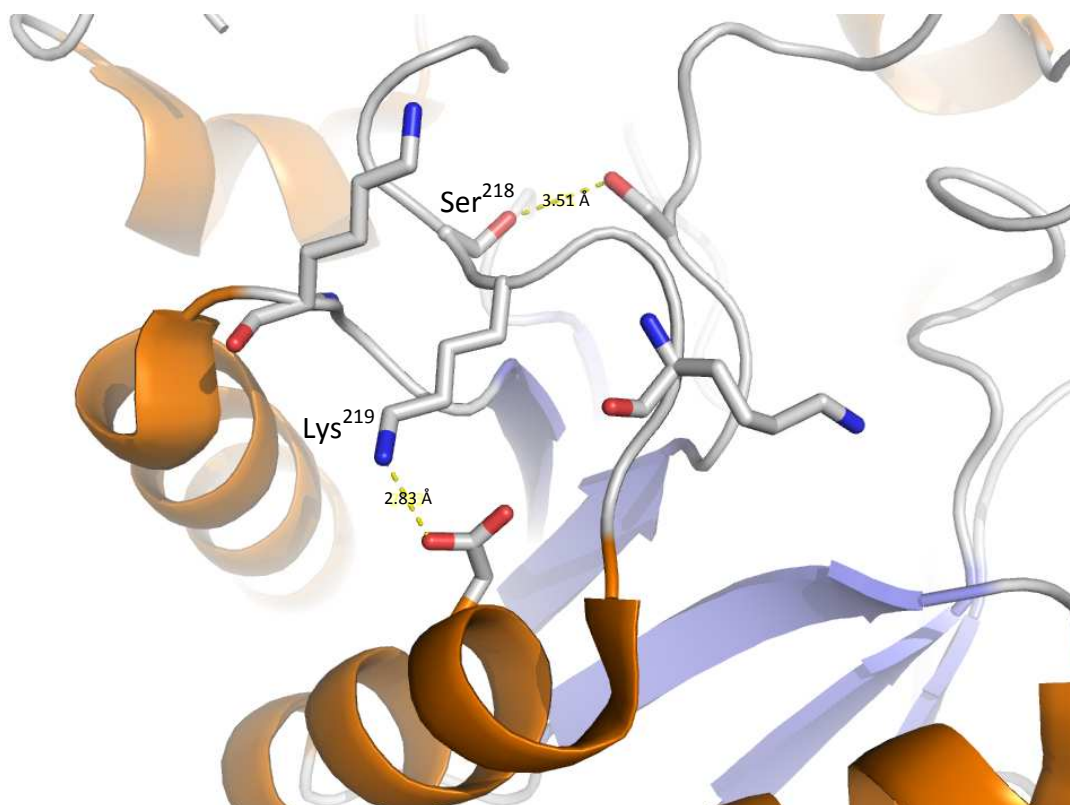


Figure 6: Ser²¹⁸ and Lys²¹⁹.

Attempts to improve the operational stability of LOX in biosensors

L-Lactate oxidase is used in biosensors. For different purposes biosensors are developed to measure also other analytes than L-lactate in one single device [30]. Hence, it can be logically concluded that certain operational conditions meeting the requirements of all employed enzymes are necessary.

In this context it was found out that the presence of carbonate has a negative impact on the stability of LOX. Therefore, the improvement of the stability is desired. Molecular dynamics simulation of LOX in the presence of 100 mM carbonate was performed by Dr. Rene Meier and suggested an accumulation of carbonate in the region of the loop where both aa, Ser²¹⁸ and Lys²¹⁹ are located (not shown). This accumulation could consequently be responsible for partial defolding due to structural changes and thereby result in a loss of stability. Concluded from this theory we hoped that the PEGylation at these sites could have a positive effect on the stability in the presence of carbonate by disturbing the interaction of carbonate in this region.

COMPREHENSIVELY EXPLICATED AND ADDITIONALLY USED MATERIALS AND METHODS

In this section the applied methods and used materials are explained or listed in more detail than above. Moreover, additional used methods not already mentioned before are described.

Materials

Strain, plasmid and primers

The vector pLO-1 shown in Figure 7 was acquired from Roche Diagnostics. Its major features are an amp resistance and the ORF encoding for LOX WT regulated by a *tac* promoter. As

transformation and expression strain *E. coli* BL21 (DE3) was used. Its chromosomal genotype is *E. coli* B dcm ompT hsdS(rB-mB-) gal.

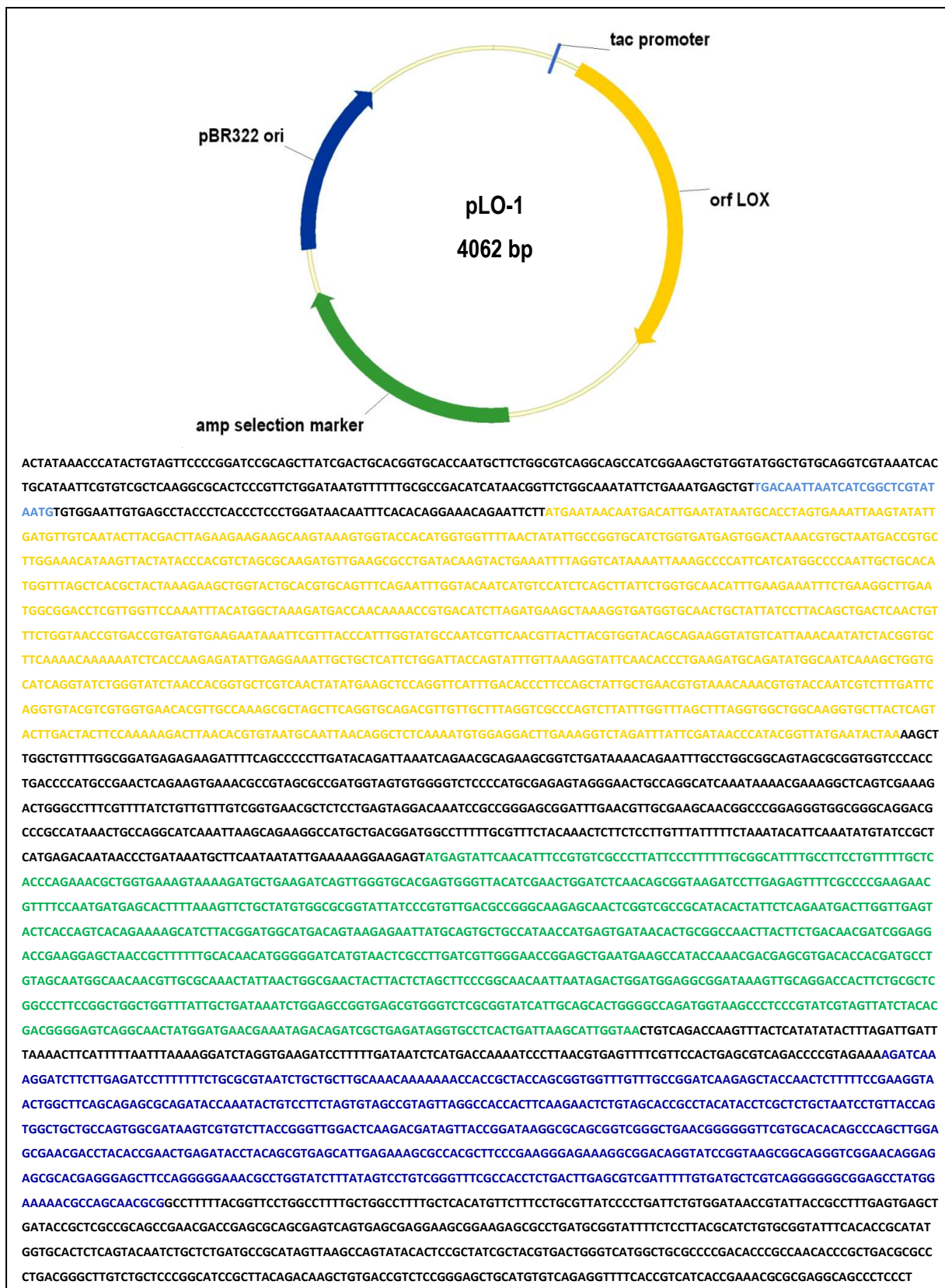


Figure 7: pLO-1 vector and sequence.

The aa sequence of LOX WT is shown in Figure 8. The mutated aa are indicated in red.

MNNNDIEYNAPSEIKYIDVVNTYDLEEEASKVVPHGGFNYIAGASGDEWTKRANDRAWKHKLLYPRLAQDVEAPDTSTEILG
 HKIKAPFIMAPIAAHGLAHATKEAGTARAVSEFGTIMSISAYSGATFEEISEGLNGGPRWFQIYMAKDDQQNRDILDEAKGD
 GATAIILTADSTVSGNRDRDVKNKFVYYPFGMPVQRYLRGTAEGMSLNNIYGASKQKISPRDIEEIAAHSGLPVFVKGIQHPED
 ADMAIKAGASGIWVSNHGARQLYEAPGSFDLPAIAERVNKRVPVFDSGVRRGEHVAKALASGADVVALGRPVLFGLALG
 GWQGAYSVLDYFQKDLTRVMQLTGSQNVEDLKGLDLFDNPPYGYEY-

Figure 8: Amino acid sequence of LOX WT.

Primers used for introducing the site-directed mutation (K219C) and sequencing purposes were purchased from Integrated DNA Technologies Inc. and are listed in Table 2.

Table 2: Used oligonucleotides for site-directed mutagenesis 2.

Primername	Sequence	T _m [°C]
K219Cfw	5`-GGTGCTTCATGCAAAAAATCTCACCAAGAGATATTG-3`	62.1
K219Crev	5`-TTTTTGGCATGAAGCACCGTAGATATTGTTAATGACATACC -3`	62.3
SeqLOX1fw	5`-GCAAGATGTTGAAGCGCCTGATAC-3	58.6

DNA bases responsible for the desired mutations are indicated in red. The introduction of silent mutations as indicated in green was not further utilized.

A comprehensive list of used instruments and devices is shown in Table 3.

Table 3: Instruments and devices.

Instrument/Device	Supplier
AEC column	Mono Q™, GE Healthcare Life Sciences
Agarose gel accessories	Chamber Mini-Sub Cell (BIORAD); Model 200/2.0 Power Supply (BIORAD)
Autoclaves	Varioklav; Fedegari; Systec; Certoklav
Beakers	Schott Duran®, Germany
Centrifuges	Eppendorf 5804R, Germany; Eppendorf 5415R, Germany; Biofuge Pico, Heraeus Instruments GmbH; Sorvall® Evolution RC Superspeed with AFM™
Cold storage room	Lassacher Großküchen, 4 °C
Cuvettes (light path 10 mm)	Plastic: Sarstedt AG & Co., Germany; Quartz: Hellma® GmbH & Co. KG

Desalting column	NAP™ column, GE Healthcare Life Sciences
Electrotransformation accessories	MicroPulser™, BIO-RAD, USA; Electroporation Cuvettes (2mm electrode gap), PEQLAB Biotechnologie GmbH, Germany
Fermenter and accessories	B. Braun Biotech International Biostat®C, Type CT5-2 Biostat®CT, Innova Air Tech Instruments 1313 Fermentation Monitor
Filters 0.2 µm	Cellulose acetate-filter and Sartolon Polyamid, Sartorius Stedim Biotech GmbH, Germany; Syringe filter PES, VWR International, GmbH
Flasks	Schott Duran®, Germany; Ilmabor® TGI, Germany; SIMAX®, Czech Republic
FPLC system	ÄKTA, Amersham Biosciences UPC-900 P-920
Freezer	Elin & Liebherr (-25 °C), Thermo Scientific Revco Legaci (-70 °C)
French press	American Instruments Company, AMINCO
Glass bottles	Schott Duran®, Germany
Glucose testing stripes	Diabur Test 5000, Roche Diagnostics
HIC column	Phenyl Sepharose™, Fast Flow, GE Healthcare Life Sciences
Incubator 37 °C	Heraeus® Instruments GmbH
Laminar flow	BIOAIR® Euroclone® Group, Aura 2000 M.A.C.4, Italy
Magnetic stirrer	Heidolph MR 3001K; Heidolph MR3000D
Microplate 96-Well, flat bottom, black	Greiner Bio-One GmbH
Native gels	Mini-PROTEAN® TGX 4-20% resolving gel (BIORAD); Mini-PROTEAN® Tetra Cell (BIORAD)
Oxygen sensor	Microx TX3 sensor, PreSens
PAGE accessories	BIO-RAD Power Pac™ Basic; BIO-RAD Mini Protean® Tetra System
PCR machines	iCycler, BIO-RAD, USA
PCR tubes	Sarstedt AG & Co., Germany
Petri dishes	Sarstedt AG & Co., Germany
pH-measurement	Biotrode electrode, Hamilton Bonaduz AG; Metrohm 691 pH-meter, METROHM AG
Photometer	Varian Cary® 50 Bio UV-Visible Spectrophotometer
Pipette tips	Ultratip Greiner Bio-One 200 µL/1000 µL
Pipettes	Pipetman P20N Gilson Inc., USA; Pipetman P200N Gilson Inc., USA; Pipetman P1000N Gilson Inc., USA; Finnpiquette 10 µL Thermo Fisher Scientific
Plate reader	Fluostar Omega, BMG Labtech
Reaction tubes 1.5 mL	Sarstedt AG & Co., Germany

Scales	Acculab vicon/Analytic, Sartorius Stedim Biotech GmbH, Germany
SDS gels	SDS PhastGel™ Gradient 8-25, GE Healthcare Life Sciences; Pharmacia High Speed Electrophoresis System, Pharmacia Biotech
SEC column	Superdex™ 200, GE Healthcare Life Sciences
Shaker	Pilot Shake®, Adolph Kühner AG, Switzerland (37 °C) Infors AG Type RC-406 HAT (30 °C)
Syringes	B. Braun Injekt®, Germany
Thermomixer	Eppendorf compact, Germany; Eppendorf comfort, Germany
Tubes 15 mL/50 mL	Sarstedt AG & Co., Germany
Vivaspin 500, 6, 20	10 kDa cutoff, Vivascience AG, Hannover, Germany
Vortex	REAXtop, Heidolph Instruments GmbH & Co. KG
Water bath	Julabo F12/Julabo25, Labortechnik GmbH, Germany
Water purification system	TKA Wasseraufbereitungssysteme GmbH, Germany

All used chemicals and suppliers are listed in Table 4.

Table 4: Reagents and suppliers.

Reagent	Supplier
(S)-(+)-2-Hydroxy-3-methylbutyric acid	Sigma-Aldrich Corp.
(S)-2-Hydroxybutyric acid	Sigma-Aldrich Corp.
(S)-2-Hydroxyisocaproic acid	Sigma-Aldrich Corp.
3,3-Dimethylglutaric Acid	Sigma-Aldrich Corp.
4-Aminoantipyrine	Sigma-Aldrich Corp.
Acetic acid	Carl Roth GmbH + Co KG
Agar	Carl Roth GmbH + Co KG
Agarose	PEQLAB Biotechnologie GmbH
Ammonium chloride	Carl Roth GmbH + Co KG
Ammonium sulfate	Sigma-Aldrich Corp.
dATP	Fermentas- Thermo Fisher Scientific Inc.
DCIP	Sigma-Aldrich Corp.
dCTP	Fermentas- Thermo Fisher Scientific Inc.
dGTP	Fermentas- Thermo Fisher Scientific Inc.
di-Potassium hydrogen phosphate	Carl Roth GmbH + Co KG
di-Sodium hydrogen phosphate	Carl Roth GmbH + Co KG

Dpnl	Promega Corp.
DTNB	Carl Roth GmbH + Co KG
dTTP	Fermentas- Thermo Fisher Scientific Inc.
EDTA	Carl Roth GmbH + Co KG
EtBr	Carl Roth GmbH + Co KG
Ethanol	Carl Roth GmbH + Co KG
Gene Ruler DNA Ladder Mix	Fermentas- Thermo Fisher Scientific Inc.
Glucose*H ₂ O	Carl Roth GmbH + Co KG
Glycerol	Carl Roth GmbH + Co KG
Glycine	Carl Roth GmbH + Co KG
Glycolic acid	Sigma-Aldrich Corp.
Guanidine hydrochloride	Carl Roth GmbH + Co KG
HEPES	Carl Roth GmbH + Co KG
HMW Protein Standard	GE Healthcare Life Sciences
Horseradish peroxidase	Sigma-Aldrich Corp.
IPTG	Carl Roth GmbH + Co KG
L-(+)-Lactic acid	Sigma-Aldrich Corp.
L-(+)-Mandelic acid	Sigma-Aldrich Corp.
LMW Protein Standard	GE Healthcare Life Sciences
Loading Dye (6x)	Fermentas- Thermo Fisher Scientific Inc.
Magnesium sulfate* 7H ₂ O	Carl Roth GmbH + Co KG
mal-mPEG2000-mal	IRIS Biotech GmbH
Miniprep-Kit	Promega Wizard® Plus SV Minipreps DNA Purification System
mPEG 5000-mal	Sigma-Aldrich Corp.
mPEG750-mal	Sigma-Aldrich Corp.
mPEG750-mal	IRIS Biotech GmbH
N,N-Dimethylaniline	Sigma-Aldrich Corp.
PCR gel purification-Kit	Macherey-Nagel NucleoSpin® Extract II Kit
Peptone	Carl Roth GmbH + Co KG
Pfu DNA Polymerase	Promega Corp.
Pfu DNA polymerase buffer	Promega Corp.
Phosphoric acid	Carl Roth GmbH + Co KG
Poly(propylen glycol)	Carl Roth GmbH + Co KG
Potassium chloride	Carl Roth GmbH + Co KG
Potassium dihydrogen phosphate	Carl Roth GmbH + Co KG

Potassium hydroxide	Merck GmbH
Roti®Quant Protein Quantitation	Carl Roth GmbH + Co KG
SDS	Carl Roth GmbH + Co KG
Sodium chloride	Carl Roth GmbH + Co KG
Sodium dihydrogen phosphate	Carl Roth GmbH + Co KG
Sodium hydrogencarbonate	Merck GmbH
Sodium hydroxide	Carl Roth GmbH + Co KG
Sodium sulfite	Carl Roth GmbH + Co KG
Thiamin	Sigma-Aldrich Corp.
Thiol Kit	Amplite™ Fluorimetric Quantitation Kit, AAT Bioquest Inc.
TRIS	Carl Roth GmbH + Co KG
Triton X-100	Carl Roth GmbH + Co KG
Yeast Extract	Carl Roth GmbH + Co KG

The compositions of all used media, buffers and primary solutions (might be combined or further diluted etc. for different applications or experiments) are listed in Table 5. Solutions which were prepared according to a reported (manufacturer's) protocol for different applications are not listed.

Table 5: Used media, buffers and solutions.

Medium/buffer/solution	Composition
Alternative substrate solutions: 400 mM (S)-2-Hydroxybutyric acid ; 400 mM (S)-(+)-2-Hydroxy-3-methylbutyric acid; 500 mM Glycolic acid; 400 mM (S)-2-Hydroxyisocaproic acid; 500 mM L-(+)-Mandelic acid	Respective substrate concentration dissolved in ddH ₂ O, pH adjusted with NaOH at 37 °C
Ammoniumsulfate 1.5 M in potassium phosphate buffer 50 mM, pH 7.0	198.2 g/L (NH ₄) ₂ SO ₄ in 50 mM potassium phosphate buffer, pH adjusted with NaOH, steril filtered 0.2 µm
Ammoniumsulfate 3 M in potassium phosphate buffer 50 mM, pH 7.0	396.4 g/L (NH ₄) ₂ SO ₄ in 50 mM potassium phosphate buffer, pH adjusted with NaOH, steril filtered 0.2 µm
Ampicillin stock 1000x	125 mg/ml dissolved in ddH ₂ O, steril filtered 0.2 µm
DCIP stock 10 mM	2.9 g/L dissolved in 50 mM potassium phosphate buffer, pH 6.5
Destain solution (protein gels)	30% Ethanol and 10% acetic acid in ddH ₂ O

Dying solution (protein gels)	PhastGel Blue R Coomassie R350 (GE Healthcare Life Sciences) stock and 20% acetic acid 1:1 (v/v)
Fermentation medium	A: 5.5 g/L (starter culture)/22 g/L (main culture) glucose*H ₂ O B: 10 g/L peptone, 5 g/L yeast extract, 5 g/L NaCl, 1 g/L NH ₄ Cl, 0.25 MgSO ₄ *H ₂ O, 1 mL/L trace elements solution, 100 µL/L PPG C: 3 g/L K ₂ HPO ₄ , 6 g/L KH ₂ PO ₄ Stated concentrations correspond to the final concentrations in the medium after the combination of separately autoclaved solutions A, B and C.
Glycerol 30%	30% glycerol (w/w) dissolved in ddH ₂ O, autoclaved
Guanidine hydrochloride 9 M (1.3x)	0.86 g/mL dissolved in 50 mM potassium phosphate buffer, pH 7.0
HEPES buffer 40 mM containing 150 mM NaCl (and optional 500 mM NaHCO ₃), pH 8.1	9.5 g/L HEPES, 8.8 g/L NaCl (and 42.0 g/L NaHCO ₃), pH adjusted with NaOH
IPTG 1000x	250 µg/mL dissolved in ddH ₂ O, steril filtered 0.2 µm
LB	10 g/L peptone, 5 g/L NaCl, 5 g/L yeast extract, autoclaved
LB-amp	LB + 1 mL ampicillin stock solution (1000x)/L, steril filtered 0.2 µm
LB-amp-agar	LB containing 18 g/L agar, autoclaved + 1 mL ampicillin stock solution (1000x)/L, steril filtered 0.2 µm
Native/(SDS-)PAGE running buffer	30.3 g/L TRIS-base, pH 8.3, (10.0 g/L SDS), 144.0 g/L glycine dissolved in ddH ₂ O
PEG reagent stock 5 mM or 10 mM	Different PEG reagent's concentration according to the respective molecular weight dissolved in 50 mM potassium phosphate buffer, pH 7.0
Potassium chloride 1 M in potassium phosphate buffer 50 mM, pH 7.0	74.6 g KCl in 50 mM potassium phosphate buffer, pH adjusted with NaOH, steril filtered 0.2 µm
Potassium chloride solution 2 M	149.1 g/L KCl dissolved in ddH ₂ O, steril filtered 0.2 µm
Potassium phosphate buffer 50 mM, pH 7.0 and pH 6.5 respectively	Mixing of 6.8 g/L KH ₂ PO ₄ and 13.1 g/L K ₂ HPO ₄ solution to adjust to the desired pH, steril filtered 0.2 µm
Preserve solution (protein gels)	10% acetic acid and 13% glycerol in ddH ₂ O
Protein native sample buffer	50 mL 20 mM TrisHCl, pH 7,4 + 50 mL glycerol + 1 g Triton X-100 + 0.09 g Bromphenol Blue

Protein SDS sample buffer	20 mM KH_2PO_4 , 6 mM EDTA, 6% SDS, 10% glycerol, 0.05% Bromphenol Blue
SOC	20 g/L peptone, 0.58 g/L NaCl, 5 g/L yeast extract, 0.18 g/L KCl, 0.625 g MgSO_4 supplemented with 3.46 g/L glucose (autoclaved separately)
Sodium chloride 150 mM in in potassium phosphate buffer 50 mM, pH 7.0	8.8 g/L NaCl in 50 mM potassium phosphate buffer, pH 7.0, steril filtered 0.2 μm
Sodium hydroxide 1 M and 0.5 M	40.1 g/L or 20.1 g/L dissolved in ddH ₂ O, steril filtered 0.2 μm
Sodium phosphate buffer 0.1 M + 1 g/L EDTA, (optionally 4% SDS) (amount of EDTA and SDS 2x)	Sodium phosphate buffer 0.1 M, pH 8.0 supplemented with EDTA (and optionally SDS)
Sodium phosphate buffer 0.1 M, pH 8.0	Mixing of 15.6 g/L NaH_2PO_4 and 17.8 g/L Na_2HPO_4 solution to adjust to the desired pH
TAE buffer 50x, pH 8.0 for agarose gel electrophoresis	242 g/L TRIS, 57.1 mL/L acetic acid, 18.6 mg/ml EDTA in ddH ₂ O
Trace elements solution	4 g/L $\text{FeSO}_4 \cdot 7 \text{H}_2\text{O}$, 1 g/L $\text{MnSO}_4 \cdot \text{H}_2\text{O}$, 0.4 g/L CoCl_2 , 0.15 g/L $\text{CuSO}_4 \cdot 5 \text{H}_2\text{O}$, 0.1 g/L H_3BO_3 , 0.2 g/L $\text{ZnSO}_4 \cdot 7 \text{H}_2\text{O}$, 0.2 g/L $\text{Na}_2\text{MoO}_4 \cdot 2 \text{H}_2\text{O}$ and 0.4 g/L FeCl_3 dissolved in 5 M HCl

In Figure 9 the molecular mass markers used for SDS and native-PAGE, respectively, are shown.

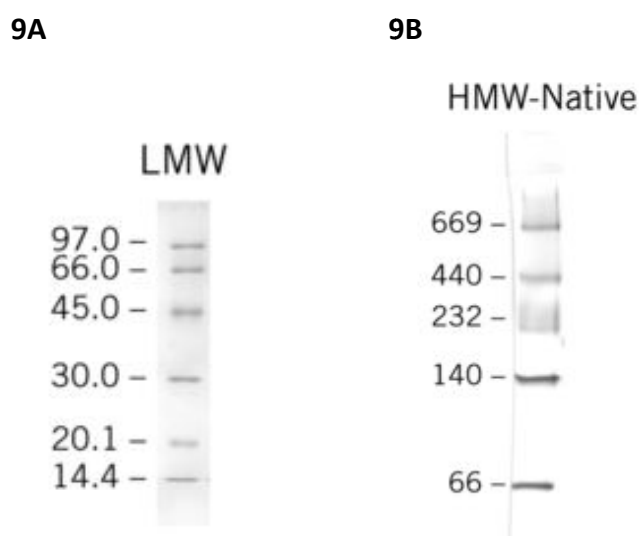


Figure 9: SDS-Low molecular weight (9A) and native-High molecular weight (9B) molecular mass markers (GE Healthcare Life Sciences).

Protein expression of mutants (cultivation in flasks)

80 mL of LB-amp medium (10 g/L peptone, 5 g/L NaCl, 5 g/L yeast extract, 100 µg/L amp) were inoculated with *E.coli* BL21 (DE3) carrying the plasmid with the respective mutation and shaken overnight at 37 °C with 130 rpm. The onc was used to generate glycerol stocks (final concentration of 15% glycerol in the stock) which were stored at -70 °C and to inoculate 200 mL LB-amp medium in a 1 L-flask to a starting OD₆₀₀ of 0.1. Cells were grown to an OD₆₀₀ of about 0.7-0.8 and then induced with IPTG to a final concentration of 250 µg/L. After 4 h of incubation at 30 °C the cells were harvested by centrifugation at 5000 rpm and 4 °C for 30 minutes. Cells were resuspended in 50 mM potassium phosphate buffer pH 7.0 and stored at -25 °C before further processing.

Protein purification

After the above described purification procedure including HIC and desalting the enzyme preparation was further purified with anion exchange chromatography (AEC) if necessary, as indicated by an unsatisfying purity detected by SDS-PAGE. The desalted HIC purified protein was loaded on the MonoQ™ column and eluted with a stepwise increasing chloride anion concentration administered from a 50 mM phosphate buffer containing 1 M KCl, pH 7.0. An overview about the entire purification procedure is shown in Figure 10.

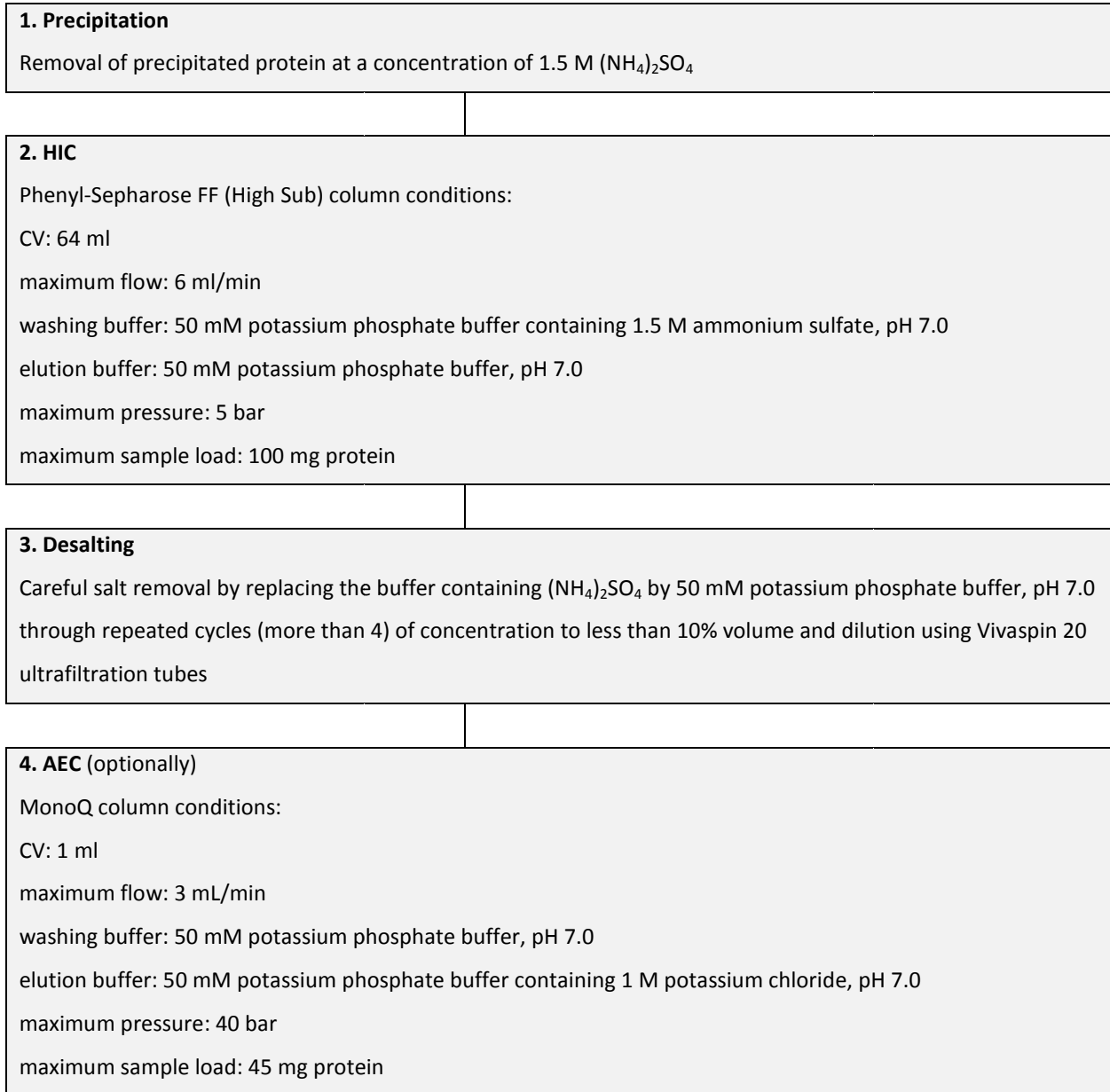


Figure 10: Purification procedure including all 4 possible steps.

Example runs of HIC and AEC are shown in Figure 11 and Figure 12, respectively. Peaks containing the protein of interest are tagged.

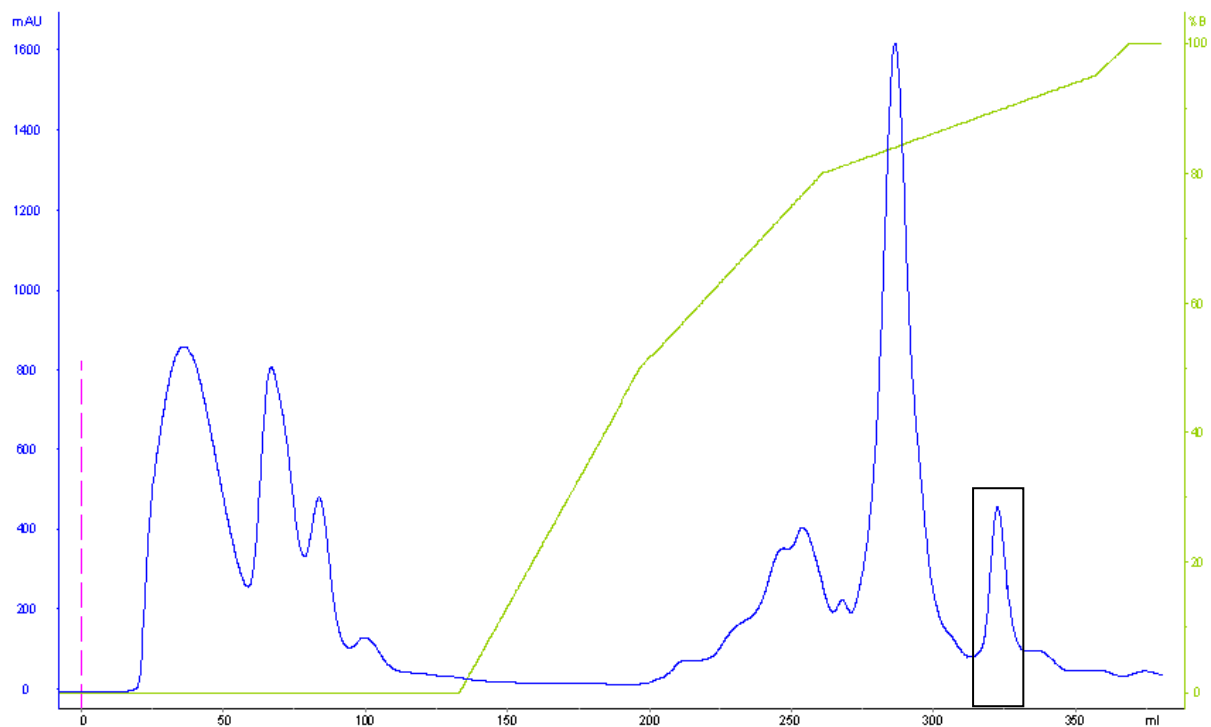


Figure 11: Example run of HIC purification with linear gradient.

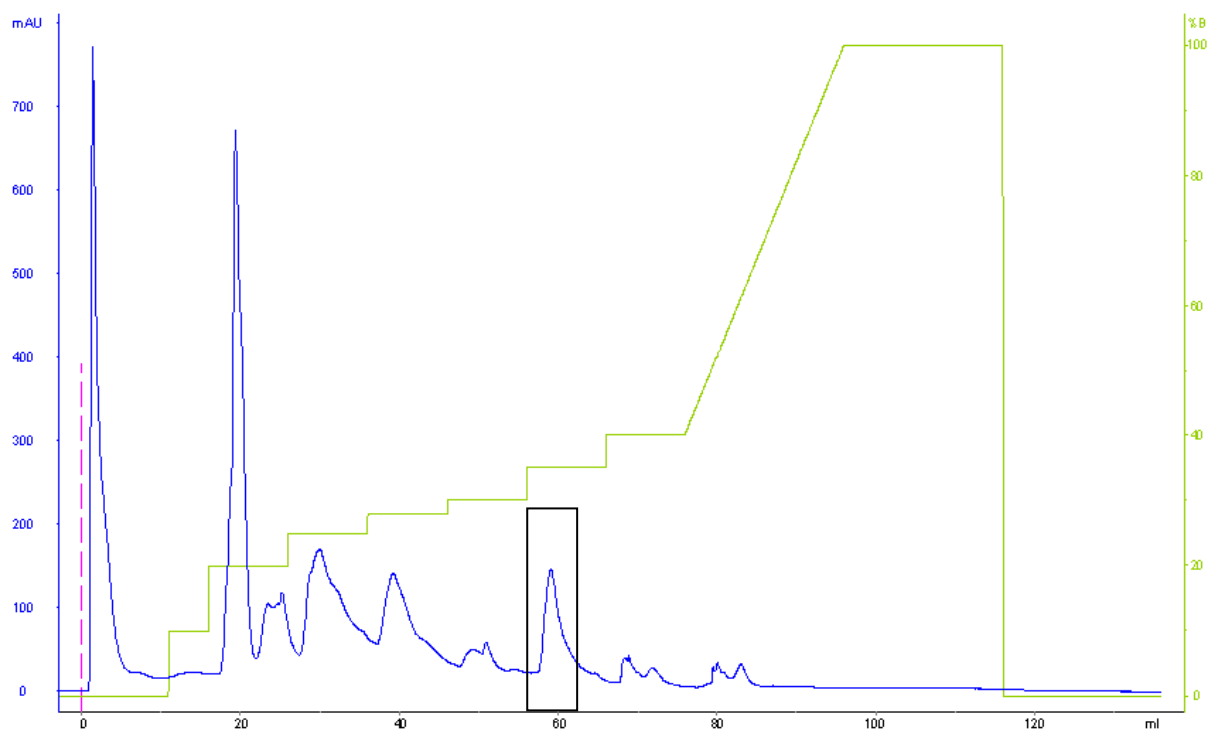


Figure 12: Example run of AEC purification with stepwise gradient.

Enzyme assays and characterization

Oxygen and DCIP measurement

O₂-measurement

Set-Up 1:

50 mM potassium phosphate buffer, pH 7.0, and substrate solution were preheated to 37 °C using a water bath. The two solutions were combined in a cuvette to a final concentration of 50 mM L-(+)-lactic acid. The mixture was stirred by a magnetic stirrer (300 rpm). Enzyme was added in an appropriate dilution. The O₂-consumption was monitored with an oxygen sensor. The temperature was assumed to be constant over the measurement time.

Set-Up 2:

In contrast to set-up 1 the buffer used was 50 mM phosphate buffer, pH 6.5. The temperature was hold on 37 °C during the whole measurement using a heating jacket assembly.

DCIP-measurement

The usage of DCIP was monitored simultaneously with the O₂-consumption of the competing reaction. DCIP acts as an alternative terminal electron acceptor. The set-up used was comparable to set-up 1 described above. Enzyme in appropriate dilution was added to the reaction mixture containing 50 mM L-(+)-lactic acid and 150 μM DCIP in potassium phosphate buffer, pH 6.5. The oxygen depletion was recorded with an oxygen sensor simultaneously to the depletion of DCIP, photometrically detected at 600 nm.

Stability

Stability in the presence of carbonate

The stability of the different enzyme preparations was also determined in the presence of carbonate. The enzyme was incubated in 40 mM HEPES containing 150 mM NaCl and 500 mM NaHCO₃ adjusted to pH 8.1. The procedure was performed as described above.

Storage stability

The enzyme was stored at 4 °C in different dilutions. The residual enzyme activity was measured with the spectrophotometric stop rate determination at different time points.

Thiol determination

Thiol determination with DTNB

Thiol determination was performed using a reported protocol with some adaptations [31]. Briefly, a 6 μM solution of native or denatured enzyme was incubated at 30 °C in the presence of a 56-338 (the amount of DTNB was varied in different experiments) molar excess of DTNB dissolved in 0.1 M sodium phosphate buffer, pH 8.0, containing 0.5 mg/mL EDTA (and optionally 2% SDS dependent on the experiment). The volume of the reaction mixture was miniaturized to a total volume of 180 μL making it suitable for plate reader measurements. The reaction was monitored after 15 min, 30 min or some h at 410/412 nm, respectively as well as continuously between 400-420 nm over 1 h.

Amplite™ Fluorimetric Thiol Quantification Kit

This method is a sensitive, one-step fluorimetric assay to detect as little as 1 picomole of cysteine in a 100 µL assay volume. The assay was performed in a 96-well black microtiter-plate according to the manufacturer’s protocol.

PEGylation

Beside the above mentioned PEGylation with mPEG-mal 5000, experiments with mPEG-mal 750 (or 840) and mal-PEG-mal with varying reactive PEG concentrations were conducted.

ADDITIONAL RESULTS AND DISCUSSION

Introduction of the mutations

The mutations Cys²¹⁸ and Cys²¹⁹ were introduced successfully into pLO-1, verified by DNA sequencing (AGOWA) as shown in Figure 13.

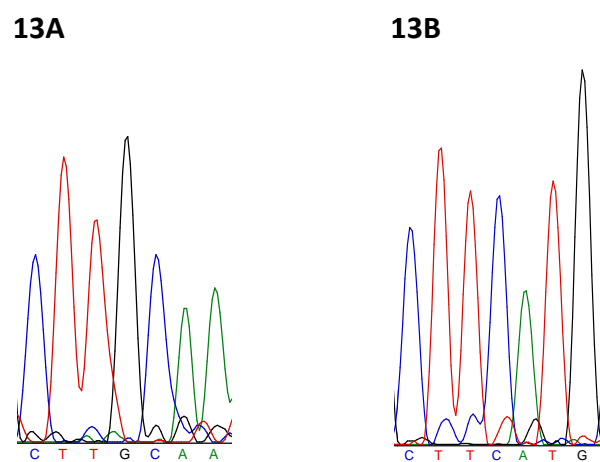


Figure 13: DNA sequences showing the mutation to Cys²¹⁸ (13A) and Cys²¹⁹ (13B).

Protein expression and purification

Expression of S218C and K219C in flasks and purification

Both enzyme mutants were successfully expressed in *E.coli* BL21 (DE3). AEC fractions containing the purified protein of interest in similar quality as determined by SDS-PAGE (shown in Figure 14 and Figure 15) and activity measurement as described in part A were pooled.

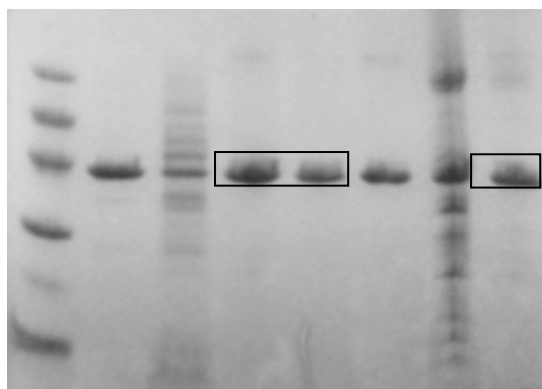
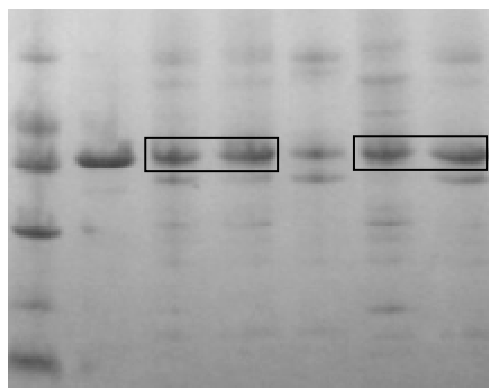


Figure 14: SDS-PAGE AEC purified S218C; lane 1, molecular mass marker; lane 2, WT (Roche Diagnostics); lane 4, 5 & 8, fractions pooled for further characterization.

15A



15B

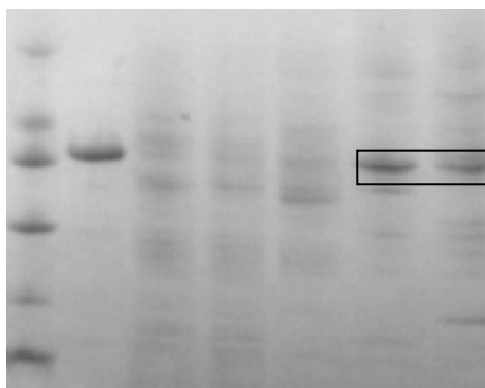


Figure 15: SDS-PAGE AEC purified K219C; lane 1 (15A and 15B), molecular mass marker; lane 2 (15A and 15B), WT (Roche Diagnostics); lane 3, 4, 6 & 7 (15A) and lane 6 & 7 (15B), fractions pooled for further characterization.

While the performed chromatography steps for the purification of S218C were reproducible (repeated runs showed comparable purity quality) the AEC purification for K219C was varying in each run performed, delivering different qualities of purified protein and being less reproducible. After all purification steps (precipitation, HIC, AEC) the yield of purified enzyme was 0.4-0.8 mg/L culture.

Addition comments to fermentation and purification of S218C

S218C was expressed and purified successfully. The final OD₆₀₀ of the fermentation was 28, the yield 33 g wet weight/L culture.

In respect of a higher yield of purified enzyme the purification procedure was completed after HIC. The yield of HIC purified enzyme was 71 mg/L culture.

Characterization and PEGylation

Specific activity for different substrates

The kinetic characteristics for the substrate L-(+)-lactic acid and a range of other substrates which are converted to the corresponding α -keto-acids by LOX are listed in Table 6, Table 7 and Table 8. The measurements were performed using the assay described in part A.

Table 6: Activity of mutants expressed in flasks.

Mutant	Substrate	Specific activity [U/mg]	k_{cat} [s ⁻¹]	K_M [mM]	k_{cat}/K_M [(s*mM) ⁻¹]
S218C	L-(+)-Lactic acid	75	52	1.3	39
	Glycolic acid	1.0	0.66	0.94	0.71
	(S)-2-Hydroxybutyric acid	2.6	1.8	4.17	0.43
K219C	L-(+)-Lactic acid	11	7.7	2.6	2.9
	Glycolic acid	0.1	0.09	3.2	0.03
	(S)-2-Hydroxybutyric acid	0.4	0.25	6.2	0.04

The specific activity for S218C for L-(+)-lactic acid is lowered by a factor of about 2.7 compared to the WT while for K219C, by a factor of approximately 18, both originating from the expression in flasks. The interaction between Lys²¹⁹ and Asp²²⁶ in the native form (shown in Figure 6) which is lacking in K219C due to the mutation might be of importance for the activity. Furthermore, the K_M of K219C is higher by a factor of 3.1. Besides, the slightly lower purity of the K219C preparation as visible on the SDS-gel must be kept in mind when discussing the significance of kinetic data. Consequently, S218C was considered to be more promising for further experiments and K219C was not further used for PEGylation studies. To obtain higher yields of S218C it was fermented in larger scale. The kinetic data for the fermented protein is summarized in Table 7. The specific activity of the fermented S218C was insignificantly higher (by a factor of about 1.2) than of the corresponding enzyme expressed in flasks. The conditions in the fermenter were optimized in regards of medium composition, oxygen partial pressure, pH and stirring, as a consequence the resulting enzyme might be of higher quality (correct folding, etc.).

Table 7: Activity of S218C expressed in fermenter.

Mutant	Substrate	Specific activity [U/mg]	k_{cat} [s ⁻¹]	K_M [mM]	k_{cat}/K_M [(s*mM) ⁻¹]
S218C	L-(+)-Lactic acid	90	62	1.0	61
	Glycolic acid	0.9	0.62	1.2	0.5
	(S)-(+)-2-Hydroxy-3-methylbutyric acid	0.03	0.02	5.1	0.004
	L-(+)-Mandelic acid	0.1	0.06	0.34	0.2

The specific activity of S218C (originating from the fermentation) for L-(+)-lactic acid is lowered by a factor of about 2.3 compared to the WT (shown in Table 7 and Table 8). The K_M for L-lactic acid of the WT is slightly lower than for the mutant. The kinetic characteristics for the other substrates are, as expected for these mutants having their mutations not in the active site but on the protein surface, not changed significantly and therefore not further discussed.

Table 8: Kinetic data of WT.

Mutant	Substrate	Specific activity [U/mg]	k_{cat} [s ⁻¹]	K_M [mM]	k_{cat}/K_M [(s*mM) ⁻¹]
WT	L-(+)-Lactic acid	204	140	0.83	167
	Glycolic acid	1.4	0.98	0.44	2.2
	(S)-(+)-2-Hydroxy-3-methylbutyric acid	0.2	0.16	3.3	0.05
	L-(+)-Mandelic acid	0.1	0.10	0.48	0.19

Oxygen measurement

The results of the oxygen measurement with L-(+)-lactic acid as substrate are summarized in Table 9.

Table 9: O₂ depletion.

Set-up	Mutant	Specific activity [U/mg]
1	K219C ^a	8.3 ± 0.2
1	S218C ^a	52.0 ± 5.0
2	S218C ^b	131.7 ± 2.5

^a expressed in flasks; ^b expressed in fermenter

The rates for the oxygen depletion in set-up 1 were approximately 30% lower than specific activities obtained via the spectrophotometric stop rate determination. The temperature during this set-up was only assumed to be constant at 37 °C where the LOX enzyme activity should be on its maximum. Lower effective reaction temperature could have resulted in the activity decrease. Besides, the oxygen depletion was monitored at pH 7.0 while the spectrophotometric stop rate determination was performed at pH 6.5. These variations were eliminated in set-up 2. Hence, the oxygen depletion is about 45% higher compared to the rates obtained with the spectrophotometric stop rate determination but can be considered to be approximately in the same range of magnitude. Further oxygen measurements to obtain more detailed characteristics were not performed.

DCIP measurement

DCIP can act as an alternative redox mediator instead of O_2 . The conversion of DCIP in a competing reaction with O_2 as electron acceptor is shown in Figure 16.

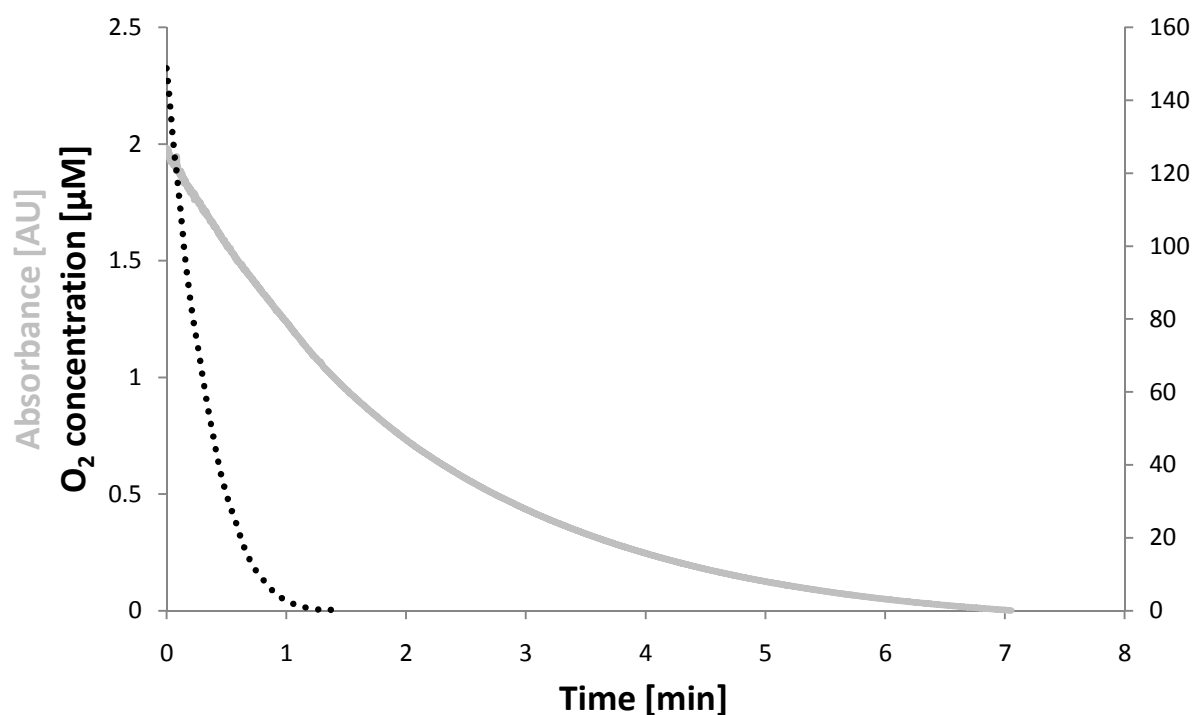


Figure 16: DCIP (full light gray line and left y-axis) vs. O_2 (broken black line and right y-axis) acting as electron acceptor.

Linearity of the depletions is only given in a very small time range. Consequently, the rates for the respective specific activities shown in Table 10 are only approximations. However, they definitely show the trend that S218C preferred O_2 over DCIP as electron acceptor (by a factor of about 4).

Table 10: O_2 vs. DCIP.

Electron acceptor	Specific activity [U/mg]
O_2	≈ 64
DCIP	≈ 16

The sum of the rates (approximately 80 U/mg) is in accordance with the specific activity of the mutant (approximately 90 U/mg) determined with the assay reported in part A. Further DCIP characteristics e.g. under anaerobic conditions were not investigated.

Thiol determination

The determination of the protein cysteine groups could not be accomplished. With the protocol described above no difference between the WT and S218C could be detected. The miniaturization might have implicated that the cysteine concentration of the samples was below the limit of detection for plate-reader measurement.

With the Amplite™ Fluorimetric Thiol Quantification Kit it was possible to calibrate with GSH in the range of 0.01-10 μ M but the cysteine group in S218C could not be detected. The addition of guanidine hydrochloride to the reaction mixture to denaturize the protein sample (to make the thiol group easier accessible) also influenced the calibration and was thus not useful.

Hence, the detection of PEGylation could not be performed via the determination of residual thiol groups. Other methods (SDS-PAGE, MALDI-TOF-MS) had to be employed.

Stability

Stability in the absence and presence of carbonate under accelerated conditions

The stabilities of the mutants K219C and S218C originating from the expression in flasks are shown in Figure 17 in comparison to the WT.

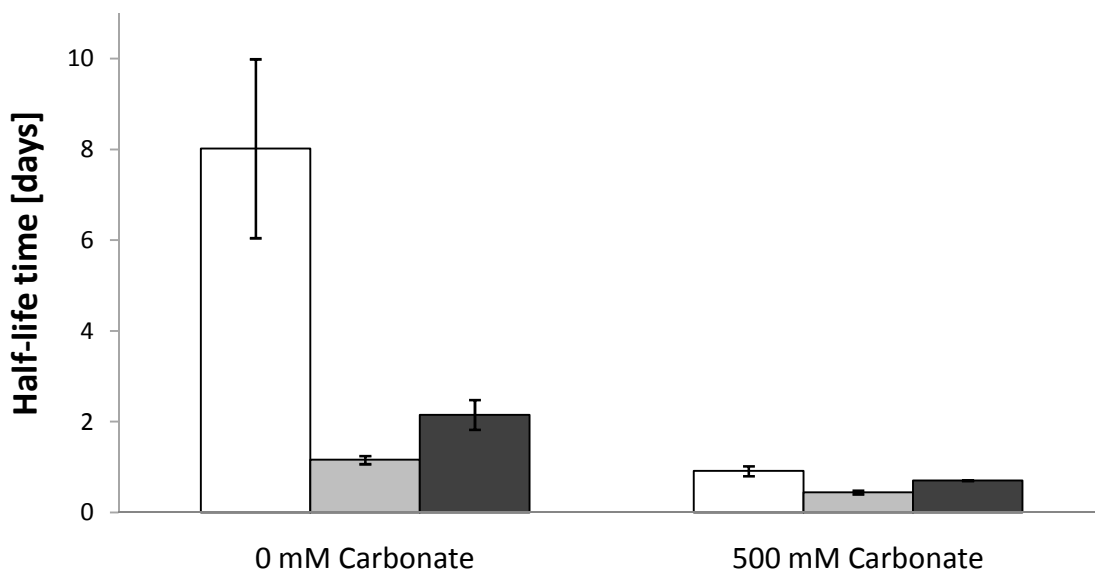


Figure 17: Stability of WT (white bars) compared to S218C (light gray bars) and K219C (dark gray bars) both originating from the expression in flasks expressed as half-life times calculated assuming pseudo-first order decay of activity determined by measuring the residual activity when incubated in 40 mM HEPES containing 150 mM NaCl, pH 8.1 at 37 °C.

The mutations destabilized the enzyme by a factor of about 3.7-6.9 and about 1.3-2.0 in the absence and presence of carbonate, respectively. The difference between the two mutants showed that the lysine mutant is slightly more stable.

Additional results from PEGylation studies

Remarks to the PEGylation with mPEG-mal 5000

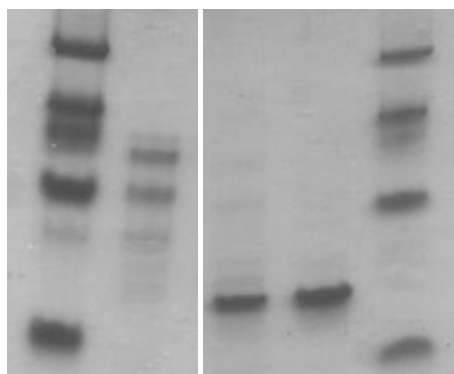


Figure 18: Native-PAGE; lane 1, native HMW molecular mass markers; lane 2, PEGylated S218C; lane 3, unPEGylated S218C; lane 4, WT; lane 5, molecular mass markers.

Already the result of the native gel suggested that the mPEG-mal 5000 PEGylated S218C was partially doublePEGylated as shown in Figure 18 and subsequently revealed by MALDI-TOF-MS analysis. (The retardation factors on the native gel of the PEGylated enzyme were not comparable to unPEGylated protein forms such as the molecular mass markers.)

Kinetic data including the characterization with additional non-natural substrates are shown in Table 11. No significant changes compared to the properties of the unPEGylated form could be observed.

Table 11: Kinetic data of PEGylated S218C.

Mutant	Substrate	Specific activity [U/mg]	k_{cat} [s ⁻¹]	K_M [mM]	k_{cat}/K_M [(s*mM) ⁻¹]
S218C	L-(+)-Lactic acid	62	43	1.03	42
	Glycolic acid	0.8	0.54	1.25	0.43
PEGylated	(S)-(+)-2-Hydroxy-3-methylbutyric acid	0.03	0.02	6.03	0.003
	L-(+)-Mandelic acid	0.1	0.04	0.65	0.07

Results of SEC (as discussed in part A) showed that the apparent molecular mass of PEGylated S218C was approximately 50-100 kDa higher than expected, assuming the presence of mono- and doublePEGylated forms of the functional tetramer of native LOX. (This was calculated by using the equation $\log(MW_{apparent}) = -0.455 * (\text{elution volume}) + 3.103$ as approximate calibration for this column derived from previous investigations done by Daniela Rainer.)

Besides the above mentioned stability studies, the stability in the presence of 500 mM NaHCO₃ under otherwise identical conditions in respect of buffer components, pH and temperature was measured. Incubated at 37 °C in 40 mM HEPES containing 150 mM NaCl and 500 mM NaHCO₃ at pH 8.1 the stability of the PEGylated S218C variant of LOX has not undergone significant changes compared to the unPEGylated form and to the WT within limits of error as shown in Figure 19. It is thus not useful for the original intended application in biosensors to overcome problems concerning stability.

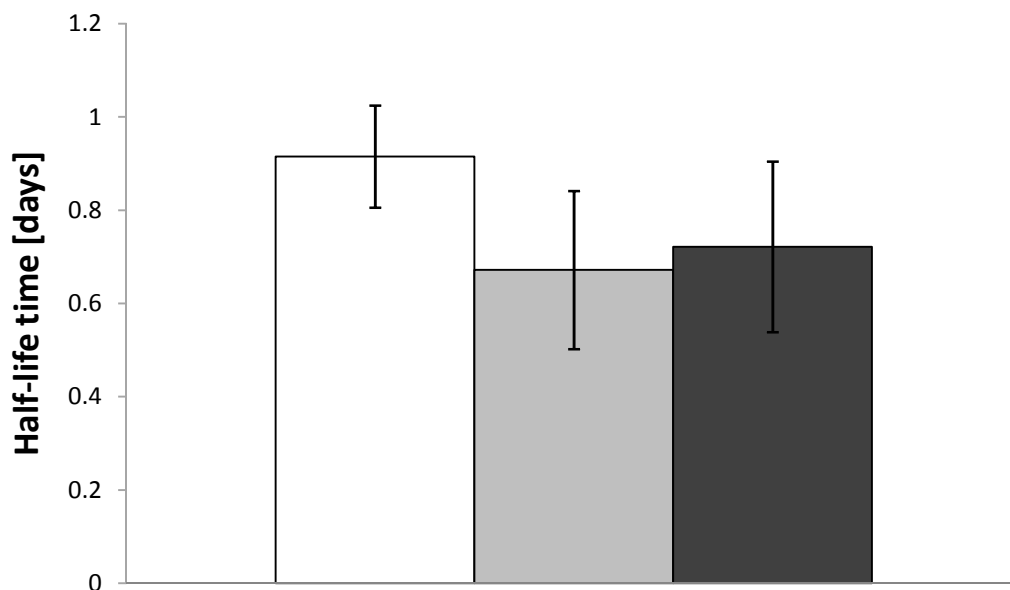


Figure 19: Stability of WT (white bar), S218C (light gray bar) and PEGylated S218C (dark gray bar) expressed as half-lives calculated assuming pseudo-first order decay of activity determined by measuring the residual activity when incubated in 40 mM HEPES containing 150 mM NaCl and 500 mM NaHCO₃, pH 8.1 at 37 °C.

The PEGylated conjugate could not be stored at -25 °C. Freezing and thawing resulted in a loss of more than 90% of activity. Hence, the mPEG-mal 5000 PEGylated S218C was stored at 4 °C and the stability under these conditions (potassium phosphate buffer, pH 7.0) was investigated as shown in Figure 20.

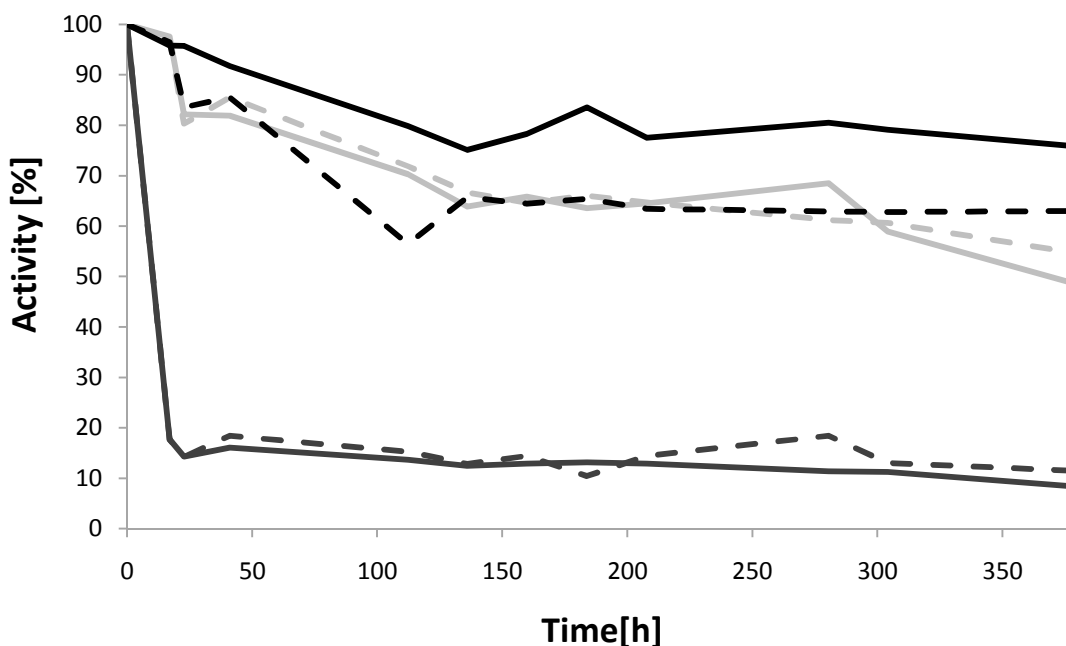


Figure 20: Storage stability of different concentrations of unPEGylated (full black line: 0.72 mg/mL; broken black line: 0.007 mg/mL) and PEGylated S218C (full dark gray line: 2.1 mg/mL; broken dark gray line: 0.42 mg/mL; full light gray line: 0.21 mg/mL; broken light gray line: 0.042 mg/mL) at 4 °C in potassium phosphate buffer, pH 7.0.

This effect has not been observed intensely but a trend could be seen. Apparently, the concentration of the PEGylated S218C had an influence on its stability and therefore residual activity. The loss of activity was significantly high at concentrations higher than 0.4 mg/mL while dilution to lower concentration helped to maintain the activity. The unPEGylated form was generally more stable and less dependent on the dilution rate.

Attempts to PEGylate S218C with mPEG-mal 750

A molecular mass increase of 7.5 (8.4) kDa couldn't be identified by SDS-PAGE. Hence, MALDI-TOF was applied to identify the product yielded when S218C was incubated with mPEG-mal 750 (Sigma) according to the procedure reported in part A. However, analysis showed that the product was not PEGylated. The same procedure was repeated in two new independent reactions. In reaction a mPEG-mal 750 (840) (IRIS Biotech) was used while in reaction b besides the same PEG reagent 100 μ M unreactive PEG 8000 was present,

hypothesizing that a longer PEG chain (as present in the successful PEGylation with mPEG-mal 5000) has positive effects on the steric accessibility of the thiol group of the cysteine. This would be an idea to explain why the reaction with the PEG reagent of higher molecular mass was successful while no PEGylation took place with mPEG-mal 750 (840). MALDI-TOF results are shown in Figure 21.

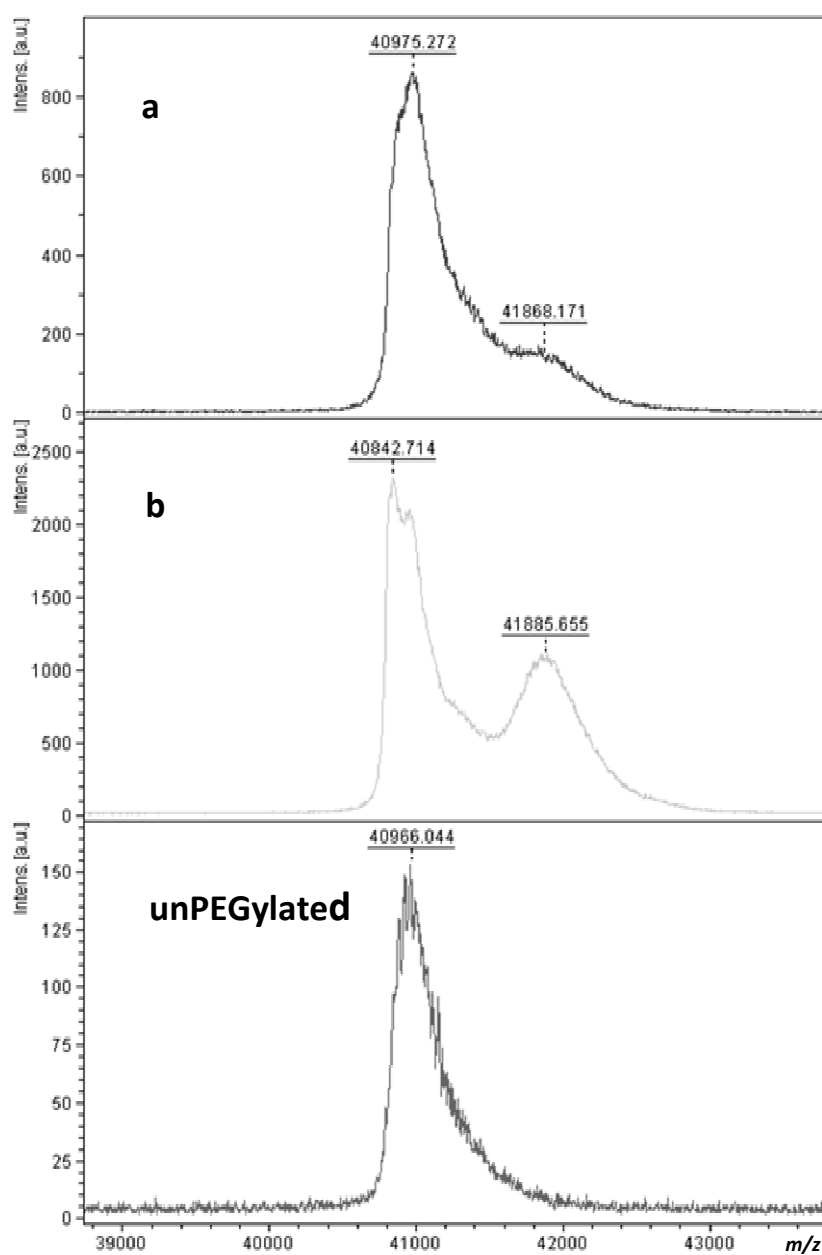


Figure 21: MALDI-TOF-MS analysis of mPEG 840-modified (a and b) and unPEGylated S218C. Details of analysis are given in part A in Supporting Information. The concentrations of the original enzyme solutions were 3.6 mg/mL and 2.0 mg/mL for a and b, respectively.

The products yielded in reactions a and b were monoPEGylated by about 20% and about 40%, respectively. The experiment was repeated, using conditions according to reaction b but the result of the previous experiment could not be reproduced. Further optimization of the reaction conditions would be necessary to ensure reproducible results. This would be very time-consuming though and was not accomplished during these studies.

Attempts to crosslink subunits of S218C with mal-PEG-mal 2000

A homobifunctional PEG reagent was used to try to crosslinking an undefined number of subunits of LOX. The enzyme was incubated according to the procedure reported in part A. Three reactions (a, b and c) differing in molar ratios of enzyme to reactive PEG reagent were set-up.

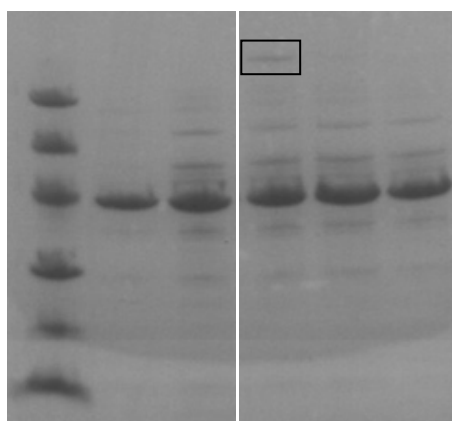
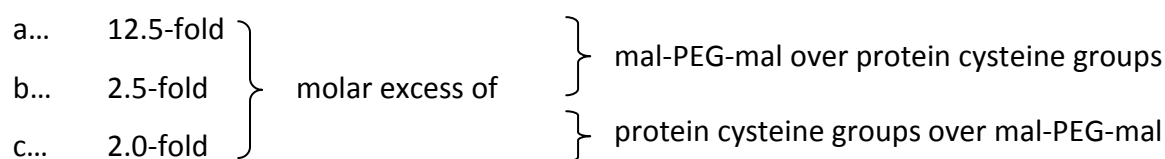


Figure 22: SDS-PAGE PEGylation; lane 1, molecular mass markers; lane 2, WT; lane 3, S218C; lane 4-6, S218C undergone PEGylation conditions a-c, respectively.

As shown in Figure 22 quantitative crosslinking could not be detected. The crosslinking might have occurred at an insignificant degree in reaction a, indicated by an apparently newly build band with an increased molecular mass. This result suggests that a greater excess of reactive

PEG reagent over protein cysteine groups might lead to PEGylation. Hence, the experiment was repeated with molar excesses of 125- and 250-fold, respectively. However, the outcome wasn't changed. An increase of molecular mass could not be identified via SDS-PAGE. The crosslinking experiments would need an intense examination and further experiments and which was not further considered in the framework of this studies.

INDICES

REFERENCES (APPENDIX)

[30] Luong, J. H., Male, K. B. and Glennon, J. D., Biosensor technology: technology push versus market pull. *Biotechnol. Adv.* 2008, 26, 492-500.

[31] Habeeb, A. F. S. A., Reaction of protein sulfhydryl groups with Ellman's reagent. *Meth. Enzymol.* 1972, 25, 457-464.

FIGURES

Part A:

TECHNICAL REPORT

FIGURE 1: OVERALL FOLD OF THE SUBUNIT OF <i>A. VIRIDANS</i> LOX (1A) AND CLOSE UP OF THE PROTEIN SITE USED FOR INTRODUCTION OF A CYSTEINE (1B); (PDB ACCESSION NUMBER: 2DU2).	8
FIGURE 2: PEGYLATION OF PURIFIED S218C MUTANT MONITORED BY SDS-PAGE (2A) AND COMPARISON OF THE VISIBLE ABSORBANCE SPECTRUM OF THE MUTATED LOX WITH THAT OF THE WILD-TYPE ENZYME (2B). 2A: LANE 1, MOLECULAR MASS MARKERS; LANE 2, UNPEGYLATED WT; LANE 3, PEGYLATED S218C; LANE 4, WT LOX UNDERGONE IDENTICAL PEGYLATION CONDITIONS; 2B: WT (BROKEN BLACK LINE) AND S218C (FULL LIGHT GRAY LINE) ABSORBANCE SPECTRA SHOWING THE CHARACTERISTIC PEAKS OF FMN IN ITS OXIDIZED FORM WERE RECORDED AT A PROTEIN CONCENTRATION OF 0.1 mM ENZYME IN 50 mM POTASSIUM PHOSPHATE BUFFER, PH 7.0 AT 25 °C.....	10
FIGURE 3: PEGYLATION OF S218C MUTANT MONITORED BY MS. PEAKS AT 41 kDA, 46 kDA AND 51 kDA, RESPECTIVELY, REPRESENT UNPEGYLATED (LIGHT GRAY LINE), MONOPEGYLATED AND DOUBLEPEGYLATED (DARK GRAY LINE) S218C FORMS. DETAILS OF MALDI-TOF-MS ANALYSIS ARE GIVEN IN SUPPORTING INFORMATION.	11
FIGURE 4: GEL FILTRATION ANALYSIS FOR S218C MUTANT AND THE PEGYLATED DERIVATIVE THEREOF. 50 µL OF 3 MG/ML SOLUTIONS OF PEGYLATED (FULL DARK GRAY LINE) AND UNPEGYLATED (FULL LIGHT GRAY LINE) LOX S218 MUTANT, RESPECTIVELY, WERE LOADED ON A SUPERDEX 200 COLUMN (GE HEALTHCARE LIFE SCIENCES) AND ELUTED ISOCRATICALLY AT 25 °C WITH 50 mM POTASSIUM PHOSPHATE BUFFER CONTAINING 150 mM NaCl, PH 7.0 WITH A FLOW RATE OF 0.5 ML/MIN AND DETECTION AT 280 NM.	12
FIGURE 5: INACTIVATION TIME COURSES FOR S218C MUTANT (LIGHT GRAY TRIANGLES) AND THE PEGYLATED DERIVATIVE (DARK GRAY CIRCLES) THEREOF IN COMPARISON TO WILD-TYPE LOX (WHITE DIAMONDS). RESIDUAL ACTIVITY IS EXPRESSED AS FRACTION OF THE STARTING ACTIVITY. THE INSET SHOWS HALF-LIFE TIMES CALCULATED FROM THE DATA ASSUMING PSEUDO-FIRST ORDER DECAY OF ACTIVITY. STABILITY OF WT (WHITE BAR), S218C (LIGHT GRAY BAR) AND PEGYLATED S218C (DARK GRAY BAR) WERE DETERMINED BY MEASURING THE RESIDUAL ACTIVITY WHEN INCUBATED IN 40 mM HEPES CONTAINING 150 mM NaCl, PH 8.1 AT 37 °C.	14

SUPPORTING INFORMATION

FIGURE S1: PURIFICATION OF S218C MUTANT DOCUMENTED BY SDS-PAGE; LANE 1, MOLECULAR MASS MARKER; LANE 2, WT LOX; LANE 3, S218C LOX CRUDE EXTRACT; LANE 4, S218C LOX AFTER (NH ₄) ₂ SO ₄ PRECIPITATION; LANE 5 AND 6, S218C LOX POOL A AND B AFTER HIC PURIFICATION.	24
----------------------------------------------------------------------------------------------------------------------------------------------------------------------------------------------------------------------------------------------------------------------------------------------------------	----

Part B:

APPENDIX

FIGURE 6: SER²¹⁸ AND LYS²¹⁹ 27

FIGURE 7: PLO-1 VECTOR AND SEQUENCE. 30

FIGURE 8: AMINO ACID SEQUENCE OF LOX WT..... 31

FIGURE 9: SDS-LOW MOLECULAR WEIGHT (9A) AND NATIVE-HIGH MOLECULAR WEIGHT (9B) MOLECULAR MASS MARKERS (GE HEALTHCARE LIFE SCIENCES). 37

FIGURE 10: PURIFICATION PROCEDURE INCLUDING ALL 4 POSSIBLE STEPS. 39

FIGURE 11: EXAMPLE RUN OF HIC PURIFICATION WITH LINEAR GRADIENT. 40

FIGURE 12: EXAMPLE RUN OF AEC PURIFICATION WITH STEPWISE GRADIENT..... 40

FIGURE 13: DNA SEQUENCES SHOWING THE MUTATION TO CYS²¹⁸ (13A) AND CYS²¹⁹ (13B). 43

FIGURE 14: SDS-PAGE AEC PURIFIED S218C; LANE 1, MOLECULAR MASS MARKER; LANE 2, WT (ROCHE DIAGNOSTICS), LANE 4, 5 & 8 FRACTIONS POOLED FOR FURTHER CHARACTERIZATION..... 44

FIGURE 15: SDS-PAGE AEC PURIFIED K219C; LANE 1 (15A AND 15B), MOLECULAR MASS MARKER; LANE 2 (15A AND 15B), WT (ROCHE DIAGNOSTICS); LANE 3, 4, 6 & 7 (15A) AND LANE 6 & 7 (15B), FRACTIONS POOLED FOR FURTHER CHARACTERIZATION..... 44

FIGURE 16: DCIP (FULL LIGHT GRAY LINE AND LEFT Y-AXIS) VS. O₂ (BROKEN BLACK LINE AND RIGHT Y-AXIS) ACTING AS ELECTRON ACCEPTOR..... 48

FIGURE 17: STABILITY OF WT (WHITE BARS) COMPARED TO S218C (LIGHT GRAY BARS) AND K219C (DARK GRAY BARS) BOTH ORIGINATING FROM THE EXPRESSION IN FLASKS EXPRESSED AS HALF-LIFE TIMES CALCULATED ASSUMING PSEUDO-FIRST ORDER DECAY OF ACTIVITY DETERMINED BY MEASURING THE RESIDUAL ACTIVITY WHEN INCUBATED IN 40 MM HEPES CONTAINING 150 MM NaCl, pH 8.1 AT 37 °C. 50

FIGURE 18: NATIVE-PAGE; LANE 1, NATIVE HMW MOLECULAR MASS MARKERS; LANE 2, PEGYLATED S218C; LANE 3, UNPEGYLATED S218C; LANE 4, WT; LANE 5, MOLECULAR MASS MARKERS. 50

FIGURE 19: STABILITY OF WT (WHITE BAR), S218C (LIGHT GRAY BAR) AND PEGYLATED S218C (DARK GRAY BAR) EXPRESSED AS HALF-LIFE TIMES CALCULATED ASSUMING PSEUDO-FIRST ORDER DECAY OF ACTIVITY DETERMINED BY MEASURING THE RESIDUAL ACTIVITY WHEN INCUBATED IN 40 MM HEPES CONTAINING 150 MM NaCl AND 500 MM NaHCO₃, pH 8.1 AT 37 °C..... 52

FIGURE 20: STORAGE STABILITY OF DIFFERENT CONCENTRATIONS OF UNPEGYLATED (FULL BLACK LINE: 0.72 MG/ML; BROKEN BLACK LINE: 0.007 MG/ML) AND PEGYLATED S218C (FULL DARK GRAY LINE: 2.1 MG/ML; BROKEN DARK GRAY LINE: 0.42 MG/ML; FULL LIGHT GRAY LINE: 0.21 MG/ML; BROKEN LIGHT GRAY LINE: 0.042 MG/ML) AT 4 °C IN POTASSIUM PHOSPHATE BUFFER, pH 7.0..... 53

FIGURE 21: MALDI-TOF-MS ANALYSIS OF MPEG 840-MODIFIED (A AND B) AND UNPEGYLATED S218C. DETAILS OF ANALYSIS ARE GIVEN IN PART A IN SUPPORTING INFORMATION. THE CONCENTRATIONS OF THE ORIGINAL ENZYME SOLUTIONS WERE 3.6 MG/ML AND 2.0 MG/ML FOR A AND B, RESPECTIVELY..... 54

FIGURE 22: SDS-PAGE PEGYLATION; LANE 1, MOLECULAR MASS MARKERS; LANE 2, WT; LANE 3, S218C; LANE 4-6, S218C UNDERGONE PEGYLATION CONDITIONS A-C, RESPECTIVELY..... 55

TABLES

Part A:

TECHNICAL REPORT

TABLE 1: KINETIC CHARACTERIZATION OF PEGYLATED AND UNMODIFIED FORMS OF S218C FOR REACTION WITH L-(+)-LACTIC ACID.13

SUPPORTING INFORMATION

TABLE S1: USED OLIGONUCLEOTIDES FOR SITE-DIRECTED MUTAGENESIS.	18
TABLE S2: PURIFICATION OF S218C MUTANT.	24
TABLE S3: SUBSTRATE SPECIFICITIES OF DIFFERENT LOX FORMS.	24

Part B:

APPENDIX

TABLE 2: USED OLIGONUCLEOTIDES FOR SITE-DIRECTED MUTAGENESIS 2.	31
TABLE 3: INSTRUMENTS AND DEVICES.	31
TABLE 4: REAGENTS AND SUPPLIERS.	33
TABLE 5: USED MEDIA, BUFFERS AND SOLUTIONS.	35
TABLE 6: ACTIVITY OF MUTANTS EXPRESSED IN FLASKS.....	45
TABLE 7: ACTIVITY OF S218C EXPRESSED IN FERMENTER.	46
TABLE 8: KINETIC DATA OF WT.....	47
TABLE 9: O ₂ DEPLETION.	47
TABLE 10: O ₂ VS. DCIP.	48
TABLE 11: KINETIC DATA OF PEGYLATED S218C.	51

SCHEMES

Part A:

TECHNICAL REPORT

SCHEME 1: REACTION OF MALEIMIDE-ACTIVATED PEG WITH THE SIDE CHAIN OF CYSTEINE..... 7

SUPPORTING INFORMATION

SCHEME S1: ACTIVITY ASSAY..... 20